

Loading-related Regulation of Transcription Factor EGR2/Krox-20 in Bone Cells Is ERK1/2 Protein-mediated and Prostaglandin, Wnt Signaling Pathway-, and Insulin-like Growth Factor-I Axis-dependent*

Received for publication, April 28, 2011, and in revised form, September 30, 2011 Published, JBC Papers in Press, November 2, 2011, DOI 10.1074/jbc.M111.252742

Gul Zaman^{†1}, Andrew Sunters[‡], Gabriel L. Galea^{§2}, Behzad Javaheri[¶], Leanne K. Saxon[‡], Alaa Moustafa^{‡3}, Victoria J. Armstrong[‡], Joanna S. Price[§], and Lance E. Lanyon[‡]

From the [‡]Department of Veterinary Basic Sciences, Royal Veterinary College, London, NW1 0TU, United Kingdom, the [§]Department of Clinical Veterinary Science, University of Bristol, Bristol BS40 5DU, United Kingdom, and the [¶]Department of Oral Biology, University of Missouri-Kansas City School of Dentistry, Kansas City, Missouri 64108

Of the 1,328 genes revealed by microarray to be differentially regulated by disuse, or at 8 h following a single short period of osteogenic loading of the mouse tibia, analysis by predicting associated transcription factors from annotated affinities revealed the transcription factor EGR2/Krox-20 as being more closely associated with more pathways and functions than any other. Real time quantitative PCR confirmed up-regulation of *Egr2* mRNA expression by loading of the tibia *in vivo*. *In vitro* studies where strain was applied to primary cultures of mouse tibia-derived osteoblastic cells and the osteoblast UMR106 cell line also showed up-regulation of *Egr2* mRNA expression. In UMR106 cells, inhibition of $\beta 1/\beta 3$ integrin function had no effect on strain-related *Egr2* expression, but it was inhibited by a COX2-selective antagonist and imitated by exogenous prostaglandin E2 (PGE₂). This response to PGE₂ was mediated chiefly through the EP1 receptor and involved stimulation of PKC and attenuation by cAMP/PKA. Neither activators nor inhibitors of nitric oxide, estrogen signaling, or LiCl had any effect on *Egr2* mRNA expression, but it was increased by both insulin-like growth factor-1 and high, but not low, dose parathyroid hormone and exogenous Wnt-3a. The increases by strain, PGE₂, Wnt-3a, and phorbol 12-myristate 13-acetate were attenuated by inhibition of MEK-1. EGR2 appears to be involved in many of the signaling pathways that constitute early responses of bone cells to strain. These pathways all have multiple functions. Converting their strain-related responses into coherent “instructions” for adaptive (re)modeling is likely to depend upon their contextual activation, suppression, and interaction probably on more than one occasion.

It is clear that normality of bone architecture, and the ability to withstand functional loads that it implies, is achieved and maintained through a process in which the cells that bring about the (re)modeling involved are responsive, in a feedback

relationship, to the strains that load-bearing engenders in the bone tissue. This strain-related control of bone architecture has been called the “mechanostat” (1). The simplicity of this functionally adaptive concept belies the complexity of the control mechanisms involved. Although the cells responsive to the earliest mechano-responsive events are almost certainly those in contact with the bone tissue (osteoblasts and osteocytes), the actual loading-related events to which they respond (strain, strain-related fluid flow, etc.) are unclear. From the many studies on mechanical regulation of bone cell behavior, it is evident that there is no unique strain sensor or dedicated strain-responsive pathway. Rather, exposure to strain-related events appears to result in activation of a number of different nonspecific signal transduction pathways. These include generation of and signaling by nitric oxide (NO) (2–5) and prostaglandins (6, 7), ERK-mediated activation of MAPK (8), the involvement of estrogen and ligand-independent activation of estrogen receptor α (9–11), signaling by insulin-like growth factor (IGF)⁴ (12–15), and mediation by the Wnt pathway (16–18).

Although many of these individual pathways are well characterized, it is the mechanisms with which they interact to provide a structurally relevant, strain-related, location-dependent, and tissue-specific response that remain elusive. To try and resolve this situation, we had previously conducted a microarray study of changes in gene expression in mouse bones that had either been loaded *in vivo* 3, 8, 12, or 24 h earlier or were in a situation of disuse (19). This study indicated differential regulation of more than 2,000 genes after loading, none of which appeared to be specific to bone or to strain.

Analysis of the pattern of gene regulation in this study by Ingenuity software indicated statistically significant relationships between the bones, the loading situation, 18 canonical signaling pathways, and 15 functions (19). In this study, we used PASTAA analysis of the genes involved in these pathways and functions. This revealed that the transcription factor EGR2/Krox-20 appeared more often in more loading-related func-

* This work was supported in part by a program grant (to L. E. L. and J. S. P.) from the Wellcome Trust.

⌘ Author's Choice—Final version full access.

¹ To whom correspondence should be addressed. E-mail: gzaman@rvc.ac.uk.

² Recipient of a training fellowship for veterinarians from the Wellcome Trust.

³ Present address: Dept. of Surgery, Faculty of Veterinary Medicine, Kafr El Sheikh University, Kafr El-Sheikh 13561, Egypt.

⁴ The abbreviations used are: IGF, insulin-like growth factor; PTH, parathyroid hormone; PASTAA, predicting associated transcription factors from annotated affinity; qPCR, quantitative PCR; SN, sciatic neurectomy; ER, estrogen receptor; PMA, phorbol 12-myristate 13-acetate; PG, prostaglandin; OVX, ovariectomy.

tions than any other despite the fact that changes in its levels of expression by the microarray had not achieved statistical significance.

EGR2 has been previously suggested to play a role in bone development because EGR2 knock-out mice are osteopenic (20). Preliminary observations supporting a role for EGR2 in adaptive bone remodeling in response to strain have subsequently been confirmed (21). Given the potential importance of EGR2 to bone homeostasis, we therefore sought to identify its role in a number of the signaling pathways already demonstrated to be utilized during bone cell response to mechanical strain.

In addition to the PASTAA analysis, which identified EGR2 as a potentially important contributor to post-loading responses of bone cells, the studies described here investigated the involvement of strain-related regulation of EGR2 with the known strain-responsive signaling pathways prostaglandins, nitric oxide, integrins, estrogen receptor, the Wnt pathway, and IGF-1. We present evidence that PKC promotes and PKA attenuates EGR2 expression and that EGR2 activation is dependent on ERK1/2 activity. Additionally, we show that although EGR2 is involved in a number of strain-related pathways within minutes of exposure to strain, it is not common to all of them because the PGE2-related down-regulation of the soluble Wnt antagonist SOST is unaffected by silencing strain-related regulation of EGR2.

EXPERIMENTAL PROCEDURES

Materials—Dulbecco's minimal essential medium (DMEM) without phenol red, L-glutamine, penicillin/streptomycin, trypsin/EDTA, and phosphorylated focal adhesion kinase Y397 rabbit monoclonal antibody were purchased from Invitrogen. Heat-inactivated fetal calf serum was purchased from LabTech International (East Sussex, UK). RNeasy mini kit, QIAshredder columns, QiaZol lysis reagent, and SYBR Green were purchased from Qiagen (Crawley, UK). PMA and SNAP2 were purchased from Calbiochem. 17β -Estradiol, LiCl, PGE2, AH8609, AH23848, collagen, fibronectin and hPTH(1–34) were purchased from Sigma. ICI 182,780, H89, NS398, dibutyl cyclic AMP, echistatin, and L-NAME were purchased from Tocris (Bristol, UK) and IGF-1 analog (des-(1–3)-IGF-1) was purchased from GroPep, Adelaide, Australia. Protran nitrocellulose membranes were purchased from Schleicher & Schuell. Superscript II reverse transcriptase was purchased from Invitrogen. EGR2 antibody was purchased from Santa Cruz Biotechnology (La Jolla, CA). Fluorescein isothiocyanate-conjugated goat anti-mouse or goat anti-rabbit IgG was purchased from Dako (Ely, UK).

Treatments in Vivo—The purpose of the *in vivo* experiment was to establish the effects on *Egr2* expression of estrogen receptor signaling pathways. To assess the effect of the estrogen receptor on *Egr2* expression, a group of 17-week-old C57BL/6 female mice were injected with the ER blocker ICI 182,780 (4 mg/kg/day) subcutaneously for 21 days to test the potential role of estrogen and signaling on *Egr2* mRNA expression levels assessed.

Mechanical Loading in Vivo—The right tibiae of 15-week-old female C57BL/6 mice ($n = 32$) and a separate group of

unilaterally sciatic neurectomized mice, in which the tibiae received no functional loading (the WT-SN group), were subjected to a single period of dynamic axial loading using a hydraulic actuator under feedback control (Dartec HC10, Zwick Testing Machines Ltd., Leominster, UK) to produce a peak compressive strain of -1300 microstrain ($\mu\epsilon$) on the medial surface of the bone at a frequency of 2 Hz for 30 s (2 Hz). In previous studies, this regimen, which included the previous microarray study (19), proved sufficient to produce an osteogenic response (19, 22). The contralateral limb was not loaded and served as an internal control (23). Eight animals were sacrificed at each time point of 3, 8, 12, and 24 h after loading.

Cell Culture—To assess the effects of strain on EGR2 expression in primary osteoblast-like cells, cultures of these were prepared from the long bones of 17-week-old female high bone mass mice (LRP5^{G171V}) and their wild-type littermates as described previously (15). These osteoblast-like cells, and the UMR106 cells also used in these studies, were seeded in complete media (Dulbecco's modified Eagle's medium without phenol red supplemented with 10% (v/v) fetal calf serum, 2 mM L-glutamine, 100 units/ml penicillin, and 100 $\mu\text{g/ml}$ streptomycin) at a density of 8×10^3 cells/cm² onto 66-mm dishes for treatment with exogenous agents or onto plastic slides (when subjected to mechanical strain). 100-mm dishes used for the integrins experiment were coated with collagen and fibronectin and air-dried prior to use.

Mechanical Straining in Vitro—Osteoblast-like cells cultured on plastic slides were subjected to a single period of 600 cycles of four-point bending at a frequency of 1 Hz. The waveform of each strain cycle consisted of a ramped square wave with strain rates on and off of 23,000 $\mu\epsilon/s$, dwell times on and off of 0.4 and 0.75 s, respectively, and a peak strain of 3,400 $\mu\epsilon$ (15). Following strain treatment, the cells were maintained in the media exposed to the strain and cultured for specified times after treatment. Controls and treated cells on slides and in wells or dishes were maintained under similar conditions.

Treatments in Vitro—In the case of pretreatment, compounds were added to the cultures of primary osteoblast-like cells or cells of the UMR106 cell line 3 h prior to stimulation with strain. To test the effects of the estrogen receptor, monolayers of osteoblast-like cells were cultured in the presence of estrogen (10^{-8} M) and ICI 182,780 (10^{-7} M). When the effects of hPTH(1–34) were investigated, the hormone was added at a final concentration of 0.01 or 10 nM for 1 h. To test the potential role of integrin and nitric oxide-mediated signaling, cells were cultured in the presence of echistatin (100 nM) (24) and SNAP2 (100 μM), respectively. PGE2 (5 μM) and prostaglandin receptor antagonists (AH6809 (30 μM) and AH23848 (30 μM)) were used to assess the contribution of prostaglandin signaling pathways. PMA (500 nM) was used as a PKC agonist, and dibutyl cyclic AMP (1 mM) and H89 (1 μM) were used as PKA agonist and antagonist, respectively. IGF-1 analog (des-(1–3)-IGF-1), when present, was added at a final concentration of 50 ng/ml.

Total RNA Isolation from Mouse Bones and Osteoblast-like Cells in Monolayer Cultures—Right and left tibiae were carefully dissected, and all their surrounding musculature was removed leaving the periosteum intact. The cartilaginous ends of the bones were removed, and the remaining tibial shaft was

EGR2 in Loading-related Gene Regulation in Bone Cells

TABLE 1
Quantitative real time RT-PCR primer sequences (5' → 3')

Gene	Sequence (forward)	Sequence (reverse)	Position	Length	GenBank™ accession no.
<i>Egr2</i>	CGCCACACCAAGATCCAC	AGCCCCAGGACCAGAGG	1586–1682	96	NM_010118
<i>Ep1</i>	CTGCTGGTATPGGTGGTG	GGTAGGAGCGAAGAAGTTG	1530–1693	163	NM_013110
<i>Ep2</i>	ACGAAAGCCAGCCATCA	CCAGCGGATGAGGTTTC	110–175	65	NM_013088
<i>Ep3</i>	ACTGTCGGTCTGCTGGTC	CCTTCTCCTTTCCCATCT	854–968	114	NM_012704
<i>Ep4</i>	ACATGGGCGTGGGTAGGT	GTGGTCCAGTCGATGAAGCA	464–527	63	NM_032076
<i>Oc</i>	CATGAGGACCTCTCTCTGC	TGGACATGAAGGCTTTGTCA	798–893	109	NM_013414
<i>Ho-1</i>	GGTGTCCAGGAAGGCTTTAAG	GTGCAGCTCCTCAGGAAGTAG	239–386	129	NM_012580
<i>Igf-1</i>	TCACATCTCTTCTACCTGGCACTC	CAGTACATCTCCAGCCTCCTCAGA	71–309	238	NM_178866
<i>Actb</i>	CTATGAGCTGCCTGACGGTC	AGTTTCATGGATGCCACAGG	798–912	114	NM_031144
<i>B2m</i>	ATGGCTCGCTCGGTGACCTT	TTCTCCGGTGGGTGGCGTGA	52–161	109	NM_0039735

spun at 5,000 rpm for 2 min (Eppendorf centrifuge) to remove the marrow. The tibial shafts were then snap-frozen in liquid nitrogen, pulverized under liquid nitrogen using a mortar and pestle, and lysed in QIAzol lysis reagent. Total RNA from these lysed samples was purified and DNase-treated using the RNeasy mini kit according to the manufacturer's protocol. Total RNA from osteoblast-like cells was isolated and DNase-treated using RNeasy Plus mini kit. The quantity and the integrity of the purified RNA were assessed using the Agilent RNA Bioanalyzer (Agilent Technologies UK Ltd., Stockport, UK).

Quantitative Real Time RT-PCR—*Egr2* mRNA expression levels were analyzed using quantitative real time RT-PCR (RT-qPCR). Total RNA was reverse-transcribed with Superscript II reverse transcriptase. Real time qPCR was carried out as described earlier (25) using QuantiTect SYBR Green PCR kit and Opticon 2 LightCycler (MJ Research, Waltham, MA). Primer sequences, the positions in the coding region, and the expected PCR products for *Egr2*, *Ep1–Ep4*, *Oc*, *Ho-1*, *Igf-1*, and the housekeeping genes (β -actin (*Actb*) and β_2 -microglobulin (*B2m*)) are summarized in Table 1. Primers for rat *Sost* were obtained from Qiagen (QuantiTect Primer Assays, QT004148558). A relative standard curve was constructed for *Egr2*, *Sost*, *Igf-1*, *Oc*, *Ho-1*, and housekeeping genes using serial dilutions of their amplicons, and these standards were included in each run. Standards were run in duplicate and samples in triplicate. Samples of unknown concentrations were quantified relative to these standard curves. The expression levels for all the genes analyzed were normalized to the reference genes (*Actb* and *B2m*). Average values were used for subsequent statistical analysis.

Luciferase Assay—UMR106 cells seeded in 6-well plates were transfected with 2.5 μ g of TCF reporter plasmid (TopFlash, Upstate Biotechnology) and 0.25 μ g of a control plasmid containing *Renilla* luciferase gene under the control of a cytomegalovirus (CMV) promoter from Promega (Southampton, UK) using TransFectin purchased from Bio-Rad or Effectene purchased from Qiagen (Crawley, West Sussex, UK). After 24 h of LiCl treatment (10 mM), the cells were washed with ice-cold PBS and lysed with 1 \times passive lysis buffer (Promega). 20 μ l of lysate was used to determine the relative luciferase activity of firefly and *Renilla* using the Dual-Luciferase assay (Promega). Firefly luciferase activity was determined and normalized to that of *Renilla*.

Immunocytochemistry—Slides or coverslips containing monolayers of osteoblast-like cells were washed in PBS, and the cells were fixed with ice-cold methanol on ice for 10 min followed by

two PBS washes. The cells were then permeabilized in buffer (20 mM HEPES, 300 mM sucrose, 50 mM NaCl, 3 mM MgCl₂, 0.05% sodium azide, 0.5% Triton X-100 (Surfact-Amps-x-100, pH 7.0)) for 10 min on ice. Nonspecific antigen-binding sites were blocked by incubating the slides in wash buffer (10% fetal calf serum, 0.05% sodium azide in PBS) for 1 h at room temperature. Slides were incubated with primary antibodies recognizing EGR2 (1:100 dilution) overnight at 4 °C in a humidified chamber, after which they were washed for 30 min at room temperature before incubation with the secondary antibody. Alexa 488-conjugated goat anti-rabbit (Molecular Probes, Invitrogen) was diluted 1:100 and incubated for 45 min in the dark at room temperature. Cells were then washed twice in wash buffer and mounted in PBS before visualization by confocal microscopy.

Western Blotting—Cells were briefly washed in ice-cold PBS and lysed in denaturing lysis buffer (2% SDS, 2 M urea, 8% sucrose, 20 mM sodium glycerophosphate, 1 mM NaF, and 5 mM Na₂VO₄) using 100 μ l/slide. Genomic DNA was sheared by passage through a QIAshredder column, and proteins and DNA denatured by boiling for 5 min. Protein concentrations were determined by the BCA assay (Perbio, Chester, UK). 20 μ g of protein were size-fractionated using SDS-PAGE and electrotransferred onto Protran nitrocellulose membranes. Membranes were blocked for 1 h in 0.2% (w/v) I-block before being incubated with primary and secondary antibodies. Proteins were visualized using the enhanced chemiluminescence detection system (ECL) (GE Healthcare). Western blots were analyzed using the ImageJ program, and band volumes were quantitated.

RNA Interference Assay—For knockdown of *Egr2*, pre-designed small interfering (si) RNA reagents were obtained using an ON-TARGETplus SMARTpool siRNA (Dharmacon, Thermo Fisher Scientific, Lafayette, CO). For transfection of siRNA, UMR106 cells were plated at 8 \times 10³ cells/cm² and left to sit overnight. The siRNA oligonucleotides were transfected the next day at a final concentration of 100 nM using Escort III transfection reagent (Sigma). UMR106 cells were treated with prostaglandin 24 h after transfection and analyzed for *Egr2*, *Sost*, and *Oc* mRNA expression by RT-qPCR. ON-TARGETplus NonTargeting siRNA pool (Dharmacon, Thermo Fisher Scientific, Lafayette, CO) was used as a negative control.

Bioinformatics—The PASTAA program was used to identify transcription factors associated with a set of co-regulated genes (26). To do this, we uploaded the data of genes differentially expressed by context (WT, WT-OVX, ER α ^{-/-}, and WT-SN)

and mechanical loading from the earlier *in vivo* microarray study (19) into PASTAA. Genes associated with a particular load-associated function were deleted from genes up-regulated by loading, and the remaining pool of genes was processed by PASTAA analysis. The p values are used as scores to subsequently rank the associations for a given transcription factor, and we assume that the smallest achieved p value corresponds to the most meaningful detectable association between a given transcription factor and a set of genes in a given category.

In addition to PASTAA we also used Whole Genome Vista analysis. PASTAA and Whole Genome Vista are two of the many analytical tools available online to identify association between a set of genes and their regulating transcription factors. PASTAA was chosen for this study because it is capable of not only recovering many known tissue-specific acting transcription factors but also provides novel associations so far not detected by alternative methods (26).

Statistical Analysis—Statistical analysis was carried out on SPSS version 17 for Windows. Up to two groups were compared by independent sample t test. Comparisons of more than two groups were made by analysis of variance with Bonferroni post hoc. Data are presented as the means \pm S.E. $p < 0.05$ was considered significant.

RESULTS

Expression of EGR2 Transcription Factor Is Regulated by Mechanical Loading—The PASTAA program analysis identified transcription factors associated with a set of co-regulated genes whose expression was perturbed by estrogen deficiency (WT-OVX), absence of estrogen receptor α ($ER\alpha^{-/-}$), and disuse because of sciatic neurectomy (WT-SN) as well as by exposure to bone loading (disuse or recent exposure to an osteogenic stimulus) superimposed on top of these contexts. For EGR2, the significance of this association was $p = 9.0 \times 10^{-6}$ for disuse (WT-SN), whereas for ovariectomy (WT-OVX) and $ER\alpha^{-/-}$ it was 0.032 and 0.033, respectively. The significance of the association for genes differentially regulated by loading at the 8-h post-loading time point was $p = 5.1 \times 10^{-5}$. A significant EGR2 positional matrix signature was observed across the conserved regions within the -10 -kb region of all the altered genes within 3 and 8 h following loading ($p < 0.001$). The affinity scores for all the genes significantly altered by loading at each time point are shown (Fig. 1A), indicating the greatest affinity scores at 8 h after loading. For further analysis, an affinity threshold (27) was arbitrarily set at 0.1 (*horizontal line* in Fig. 1A) to obtain a set of genes enriched for putative EGR2 targets. This subset of 149 genes (36% up-regulated and 64% down-regulated) was used for subsequent functional analysis. Fig. 1B shows enriched processes associated with these genes. Analysis of functional processes significantly enriched in this subset of genes using DAVID (david.abcc.ncifcrf.gov) revealed various gene ontology clusters with significantly altered components relating to the following: the cytoskeleton and cell proliferation (12 genes differentially regulated with this cluster) (Fig. 1C), cell migration (5 genes) (Fig. 1D), apoptosis (9 genes) (Fig. 1E), and motility (5 genes)

(Fig. 1F). Ingenuity Pathways analysis identified cell death/endocrine system development (Fig. 1G) and cell movement/free radical pathways (Fig. 1H) as the two most significant signaling pathways associated with these genes. Both of these pathways are related to ERK signaling.

The significance of the EGR2 association with loading-related genes was much lower when loading occurred in the context of WT-OVX ($p = 0.08$), WT-SN ($p = 0.06$), and in $ER\alpha^{-/-}$ animals lacking the gene for the estrogen receptor ($p = 0.08$).

A significance of association of EGR2 with the gene pool regulated at 8 h after loading in WT mice was assessed by sequentially deleting genes ascribed to specific functions. The more biologically significant a functionality, the less (and therefore less statistically significant) the p value becomes following the removal of the contribution of that pathway to the overall dataset. Thus, subtraction of genes for which the functionality was connected to “cellular function and maintenance” and “cellular growth and proliferation” removed the significance of the differential EGR2 footprint following mechanical loading.

In comparison to PASTAA, Whole Genome Vista analysis predicted neuronal respiratory factor 1 (NRF1), B-lymphocyte-induced maturation protein 1 (BLIMP1), and GA-binding protein as the three most over-represented transcription factors ($p < 0.005$) associated with the set of genes whose expression was perturbed by loading. PASTAA analysis results were given more weight because it is capable of not only recovering many known tissues specifically acting as transcription factors but also provides novel associations so far not detected by alternative methods.

Loading Up-regulates Egr2 mRNA Expression in Vivo—To confirm the prediction by PASTAA analysis, we used RT-qPCR to measure the changes in *Egr2* expression in the total RNA samples extracted from the loaded bones. Total RNA extracted at 3, 8, 12, and 24 h after a single osteogenic loading stimulus from 15-week-old C57BL/6 female mouse tibia (1,300 μ strain, 2 Hz, 60 cycles (19)) by RT-qPCR showed increased mRNA expression levels of *Egr2* (5.9-fold) at 3 h after loading (Fig. 2A). By 8 h after loading, *Egr2* mRNA expression levels were similar to those in controls and remained relatively unchanged until 24 h after loading.

Strain Up-regulates Egr2 mRNA Expression in Vitro in Primary Cultures of Osteoblast-like Cells and in the UMR106 Cell Line—Loading-related up-regulation of *Egr2* mRNA *in vivo* was confirmed to also occur *in vitro* in primary osteoblast-like cells derived from WT mouse long bones. These cells showed a statistically significant 2-fold increase ($p < 0.01$) in their *Egr2* mRNA expression after a single period of dynamic mechanical strain (peak strain 3,400 microstrains, 1 Hz, 600 cycles) (Fig. 2B). In this case the timing of the maximal response was at 1 h following strain, with expression levels returning to those of the controls by 3 h.

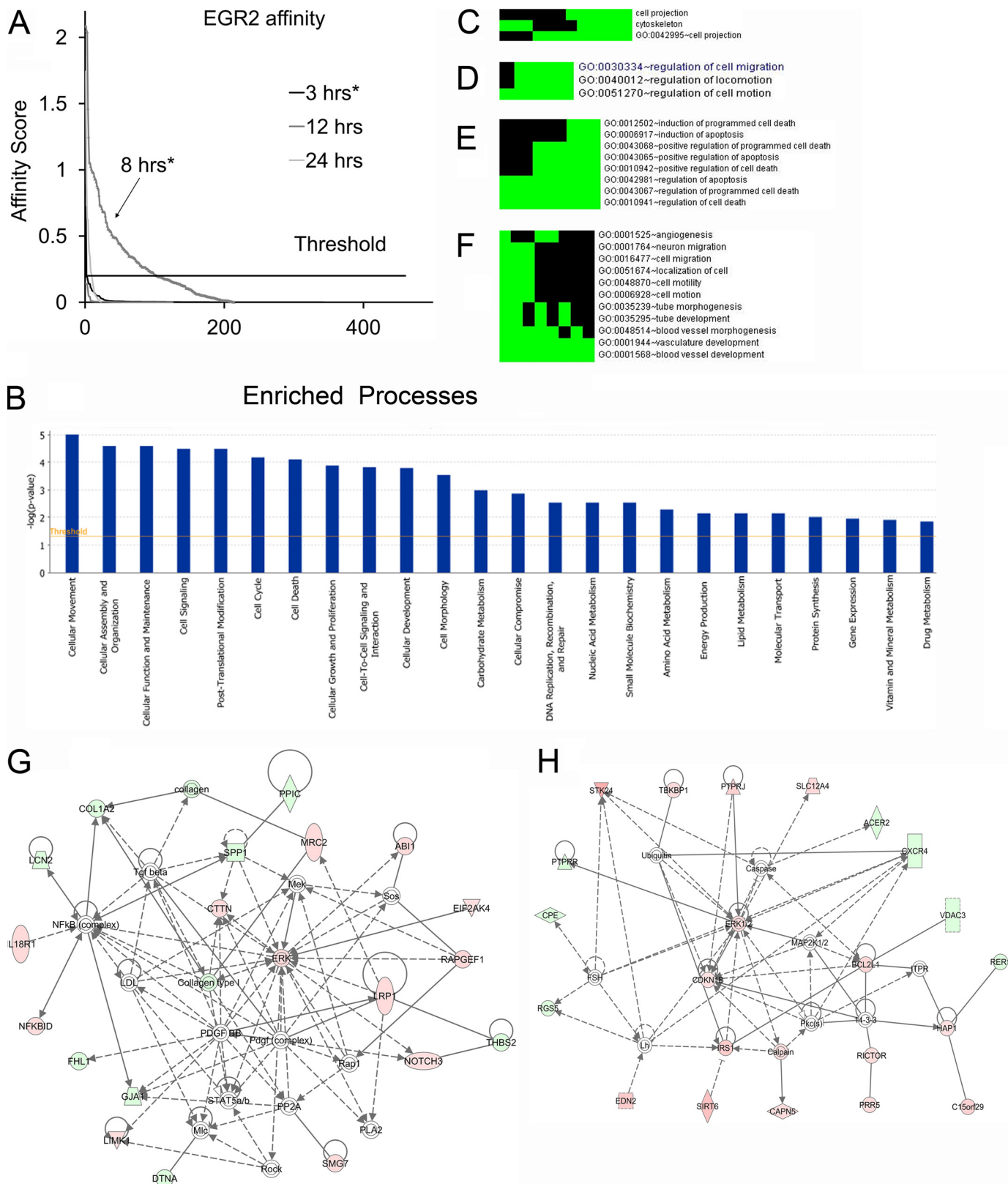
This strain-related response in primary cultures was replicated in cells of the UMR106 osteoblast-like cell line, which showed a robust 7-fold ($p < 0.001$) increase 1 h after strain (Fig. 2C). This is consistent with data from a microarray analysis in an earlier report in osteoblast cells in which tran-

EGR2 in Loading-related Gene Regulation in Bone Cells

scription of *Egr2* mRNA levels peaked at 1 h after mechanical strain (21).

Strain Up-regulates EGR2 Protein Levels That Accumulate in the Nucleus—To establish whether the strain-related increase in *Egr2* mRNA expression was translated into increased EGR2

protein, we performed Western blot analysis on whole cell lysates from UMR106 cells at various time points after the cells had been subjected to strain. Increased EGR2 protein levels visible at 1 h were maintained at all time points up to 4 h after strain (Fig. 3A). Quantitation of the levels of EGR2 relative to



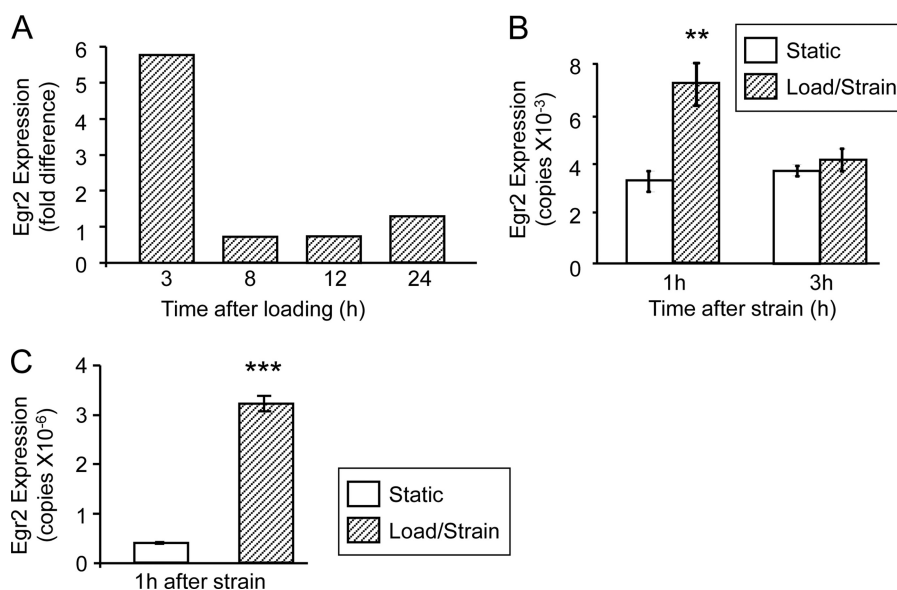


FIGURE 2. **Effect of loading on normalized *Egr2* mRNA expression.** *A*, total RNA was extracted at 3, 8, 12, and 24 h after a single period of dynamic axial loading of the mouse tibia *in vivo* and *Egr2* mRNA expression levels measured by RT-qPCR. Normalized *Egr2* mRNA expression levels are shown as fold difference compared with the nonloaded controls. *B*, primary osteoblast-like cells derived from C57BL/6 mouse long bones were seeded onto plastic strips and subjected to strain (3400 microstrain, 1 Hz, 600 cycles). Total RNA was extracted at 1 and 3 h after strain, and *Egr2* mRNA expression levels were measured by RT-qPCR. Results are shown as mean \pm S.E. **, $p < 0.01$ versus static at 1 h. *C*, UMR106 cells were seeded onto plastic strips and subjected to strain. Total RNA was extracted 1 h after strain, and *Egr2* mRNA expression levels were measured by RT-qPCR. Results are shown as mean \pm S.E. (B and C). ***, $p < 0.001$.

β -actin was performed using scanning densitometry (Fig. 3B). This demonstrated statistically significant differences at 0.5, 1, 2, and 4 h after strain. We also used immunocytochemistry associated with confocal microscopy in these cells. These techniques confirmed (Fig. 3C) increased EGR2 immunostaining 1 h after strain compared with the static control and marked accumulation of EGR2 in the nucleus.

Strain-induced *Egr2* mRNA Expression Is Not Influenced by Inhibition of Integrin Receptors—Integrins are expressed by cells of the osteoblast lineage and have been implicated in early strain-related and fluid flow-related responses of osteoblasts. To determine whether strain-related *Egr2* expression up-regulation was mediated by $\beta 1$ and $\beta 3$ integrin receptors, UMR106 cells were pretreated with the disintegrin echistatin prior to strain. Pretreatment of UMR106 cells overnight with echistatin (100 nM) had no effect on basal levels of *Egr2* expression, and the increase in *Egr2* expression following strain (3.9-fold, $p < 0.001$) was not modulated in the presence of echistatin (Fig. 4). To confirm previous reports (17, 28, 29) that echistatin was effective at inhibiting $\beta 1$ and $\beta 3$ activity, UMR106 cells were pretreated with and without 100 nM echistatin overnight, trypsinized, and then cultured on a substrate of collagen and

fibronectin for 30 min to activate the $\beta 1$ and $\beta 3$ integrins (30). This echistatin treatment effectively blocked phosphorylated focal adhesion kinase activation (Fig. 4B), a downstream target of integrin signaling (31, 32), demonstrating that $\beta 1$ and $\beta 3$ integrin function was impeded in these cells.

These data imply that strain-related *Egr2* regulation 1 h after strain does not appear to be mediated by $\beta 1$ or $\beta 3$ integrin. This does not preclude the involvement of other β -integrins.

Strain-related Increase in *Egr2* mRNA Expression Is Modulated by Prostaglandins—To assess whether strain-related increase in *Egr2* mRNA expression is modulated by PGs, UMR106 cells were strained in the presence of the selective COX2 inhibitor NS398 (1 μ M). Fig. 5A shows that NS398 had no effect on basal levels of *Egr2* mRNA expression compared with vehicle controls. However, loading-induced *Egr2* mRNA expression was abolished by pretreatment with NS398, indicating that strain-related *Egr2* regulation is mediated by prostaglandins.

To investigate the relationship between PG production and strain-related *Egr2* regulation, we treated UMR106 cells with exogenous PGE2 (5 μ M). Examination of the time course revealed that *Egr2* mRNA expression was rapidly increased by

FIGURE 1. **EGR2 is predicted to regulate loading-induced signaling networks involving ERK signaling.** *A*, PASTAA analysis was used to identify the time points following loading in which EGR2 is most closely associated with the observed transcriptional changes. A significant EGR2 positional matrix signature was observed across the conserved regions within the -10 -kb region of all the altered genes 3 and 12 h following loading (*, $p < 0.001$). The affinity scores for all the genes available at each time point are shown, indicating the greatest affinity scores at 8 h. For further analysis, an arbitrary threshold (horizontal line) was set at an affinity score of 0.1 to obtain a set of genes enriched for putative EGR2 target genes. This subset of 149 genes was used for subsequent functional analysis. Of these genes, 36% were up-regulated and 64% were down-regulated. *B*, cellular processes identified to be significantly enriched by Ingenuity pathway analysis software within this gene cluster are shown, suggesting potential functions for EGR2-regulated genes following loading. This was complemented by analysis of functional processes significantly enriched in this subset of genes using DAVID (david.abcc.ncifcrf.gov) revealing various gene ontology clusters with significantly altered components relating to the following: *C*, cytoskeleton and cell proliferation (12 genes differentially regulated in the cluster, represented by the horizontal axis); *D*, cell migration (5 genes); *E*, apoptosis (9 genes), and *F*, motility (5 genes). The number of genes pertaining to each GO term within each cluster is shown by the number of green boxes adjacent to the term, and black boxes represent genes within the cluster not yet associated with the GO term. Pathway analysis was also performed using Ingenuity Pathway Analysis. Given the small number of genes available, only the two most significantly altered pathways were studied. These pathways relate to cell death/endocrine system development (*G*) and cell movement/free radical scavenging (*H*). Both pathways relate to ERK signaling. Genes in red are up-regulated, and those in green were down-regulated.

EGR2 in Loading-related Gene Regulation in Bone Cells

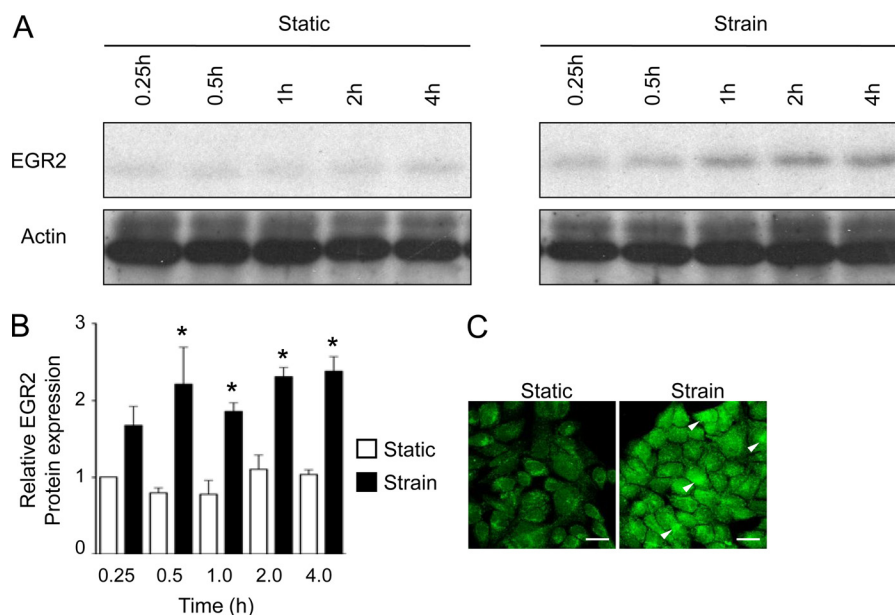


FIGURE 3. Effect of strain on EGR2 protein localization and expression. *A*, Western blot for EGR2 from whole cell lysates was prepared from static and strained UMR106 cells at 0.25, 0.5, 1, 2, and 4 h after treatment. β -Actin was used as a control for equal protein loading. *B*, scanning densitometry was performed on Western blots from three independent experiments. Values shown are mean \pm S.E. *, $p < 0.05$ versus its corresponding time point static control, paired one-tailed t test. *C*, UMR106 cells were seeded onto plastic strips, subjected to strain, and fixed 1 h later. The subcellular localization of EGR2 (green staining) was determined by immunocytochemistry and confocal microscopy. Nuclear accumulation of EGR2 in strained cells is also visible (white arrowheads). Scale bar, 20 μ m.

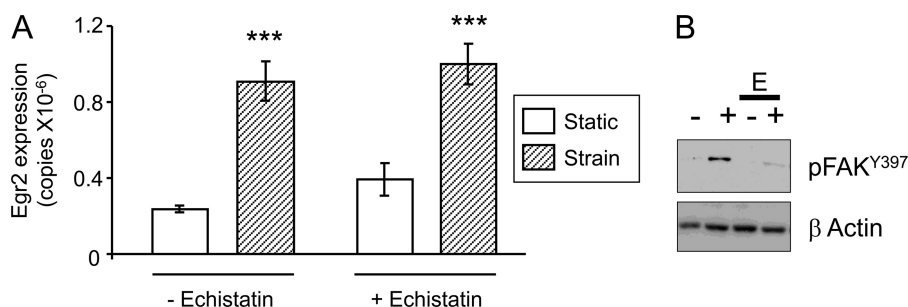


FIGURE 4. Effect of disintegrin and echistatin on strain-induced *Egr2* expression. *A*, UMR106 cells were seeded onto plastic strips and pretreated with 100 nM echistatin (disintegrin against $\beta 1$ and $\beta 3$ integrins) overnight and then subjected to a single period of strain. Total RNA was extracted 1 h after treatment, and RT-qPCR was used to measure normalized *Egr2* mRNA expression levels. Results are expressed as means \pm S.E. ***, $p < 0.001$ versus static. *B*, to show that echistatin was biologically effective in blocking the downstream effects of integrin signaling, UMR106 cells were pretreated with and without 100 nM echistatin overnight, trypsinized, and then cultured on a mixed substrate of collagen and fibronectin for 30 min to activate $\beta 1$ and $\beta 3$ integrin function. Nonadherent cells (–) were collected in ice-cold PBS, centrifuged, and lysed in denaturing lysis buffer, whereas the cells attached to the collagen/fibronectin substrate (+) were briefly washed in ice-cold PBS and lysed in denaturing buffer. Western blot for phosphorylated focal adhesion kinase (pFAK) was prepared from whole cell lysates. β -Actin was used as a control for equal protein loading.

PGE₂ treatment, reaching a maximum some 50 min after treatment and returning to basal levels by 4–6 h afterward (Fig. 5*B*). There appears to be a lag time of about an hour before a significant increase in *Egr2* mRNA expression occurs. To ascertain whether this lag time was due to the requirement of new protein synthesis resulting from the immediate signaling stimulated by PGE₂, we pretreated the cells with cycloheximide (1 μ M) for 4 h. This pretreatment did not inhibit the PGE₂-mediated increase in EGR2 expression (Fig. 5*C*) indicating that the effect of PGE₂ on *Egr2* mRNA expression is independent of *de novo* protein synthesis.

PGE₂-induced Egr2 mRNA Expression Is Mediated through EP1/2 Receptor Subtypes and PMA but Is Repressed by PKC—PGE₂ exerts its effects by acting on a group of G-protein-coupled receptors EP1–EP4. To investigate the role of these receptors in PGE₂-mediated increase in *Egr2* expression in

osteoblast-like cells, we first assessed the distribution of these receptors in UMR106 cells by PCR. *EP1* appears to be the most abundant PGE₂ receptor transcript in these cells followed by *EP2* and *EP4* (Fig. 6*A*). In contrast, basal expression of *EP3* mRNA was almost undetectable.

We next examined which EP subtype receptor (EP1, EP2, or EP4) was involved in the PGE₂-mediated increase of *Egr2* mRNA expression. PGE₂-induced increase in *Egr2* expression was abolished by blocking EP1 and EP2 receptors with AH6809 (30 μ M) (Fig. 6*B*), but inhibiting the EP4 receptor with AH23848 (30 μ M) only partially lowered its expression (by 29%, $p = 0.01$) (Fig. 6*C*).

We next investigated the effect of cAMP/PKA PKC signaling pathways on PGE₂-induced *Egr2* expression. The PKC agonist PMA (500 nM) mimicked the effect of PGE₂ on *Egr2* expression (Fig. 7*A*). The time course expression profile of

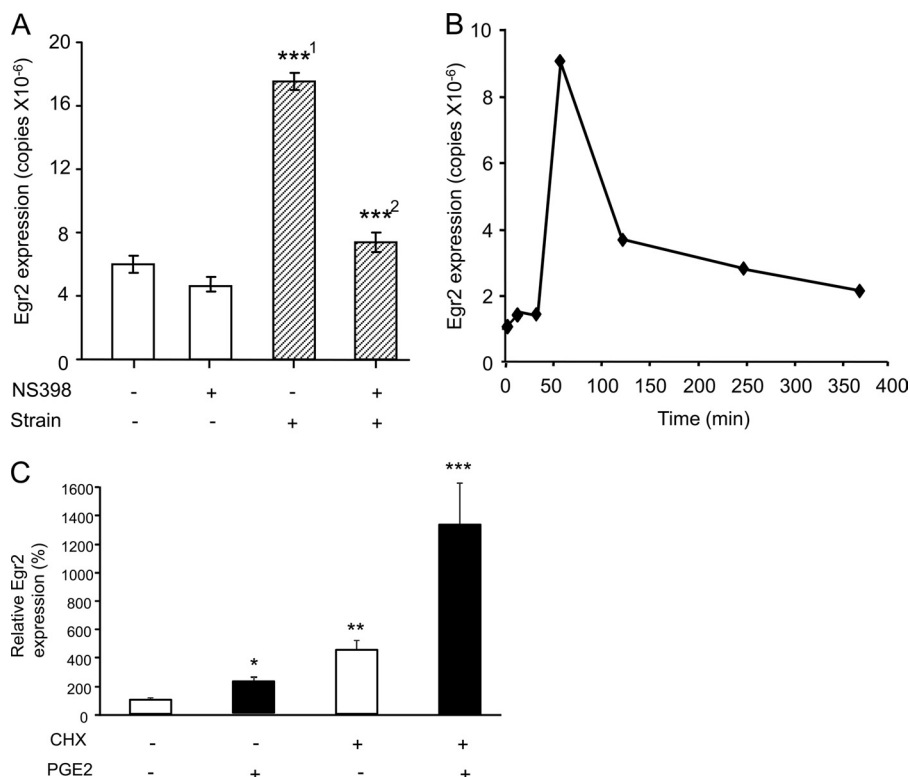


FIGURE 5. Effect of COX2 inhibitor on strain and the effect of exogenous PGE2 on *Egr2* mRNA expression. A, UMR106 cells were seeded onto plastic strips and subjected to strain in the presence or absence of 1 μM NS398 (selective COX2 inhibitor). Total RNA was extracted 1 h after strain and RT-qPCR used to measure normalized *Egr2* mRNA expression levels. Results are expressed as mean \pm S.E. ***¹, $p < 0.001$ versus static; ****², $p < 0.001$ versus strain. B, UMR106 cells were seeded in tissue culture coated dishes and treated with 5 μM PGE2. Total RNA was extracted 0, 10, 20, and 50 min and 2, 4, and 6 h after treatment, and RT-qPCR used to measure normalized *Egr2* mRNA expression levels. C, UMR106 cells were seeded on 66-mm dishes and treated with 5 μM PGE2 for 1 h in the presence or absence of 1 μM cycloheximide (CHX). Total RNA was extracted 1 h after PGE2 treatment, and RT-qPCR was used to measure normalized *Egr2* mRNA expression levels. Results are expressed as mean \pm S.E. *, $p < 0.05$ versus vehicle. **, $p < 0.01$ versus vehicle. ***, $p < 0.001$ versus cycloheximide.

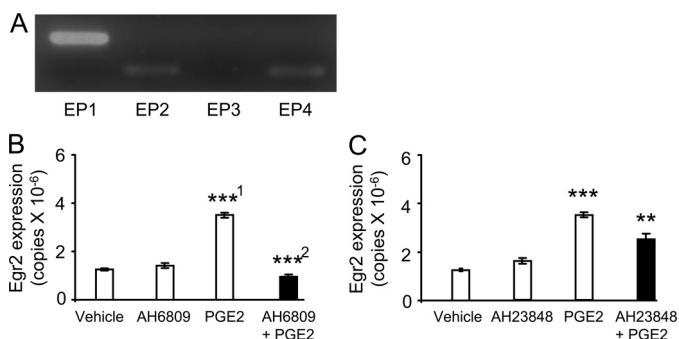


FIGURE 6. Effect of PGE2 receptor inhibitors on PGE2-induced *Egr2* mRNA expression. A, total RNA was extracted from UMR106 cells, and RT-PCR was used to amplify *EP1*, *EP2*, *EP3*, and *EP4* receptor transcripts. B, UMR106 cells were seeded on 66-mm dishes and treated with exogenous PGE2 (5 μM) in the presence or absence of 30 μM AH6809 (EP1 and EP2 receptor antagonist). Total RNA was extracted 1 h after strain, and RT-qPCR was used to measure normalized *Egr2* mRNA expression levels. Results are expressed as mean \pm S.E. ***¹, $p < 0.001$ versus vehicle; ****², $p < 0.001$ versus PGE2. C, UMR106 cells were seeded on 66-mm dishes and treated with exogenous PGE2 in the presence or absence of 30 μM AH23848 (EP4 receptor antagonist). Total RNA was extracted 1 h after strain, and RT-qPCR used to measure normalized *Egr2* mRNA expression levels. Results are expressed as mean \pm S.E. *, $p < 0.05$ versus PGE2, ***, $p < 0.001$ versus vehicle, **, $p = 0.01$ versus strain.

Egr2 in response to PMA was similar to that observed with PGE2. Exogenous treatment with dibutyryl-cyclic AMP (a stable analog of cAMP) resulted in a significant decrease in *Egr2* expression (53%, $p < 0.001$) (Fig. 7B) at 1 h after treatment. Consistent with this finding, pretreatment with the specific PKA antagonist H89 (1 μM) significantly increased

PGE2-induced *Egr2* expression (59%, $p < 0.05$) (Fig. 7C). To confirm the specificity and potency of the added H89, we measured *Igf-1* mRNA levels in response to PGE2 treatment in the presence and absence of H89. As expected, *Igf-1* mRNA expression was significantly elevated in response to PGE2 treatment, an increase that was significantly reduced by pretreatment with H89 (Fig. 7D).

Nitric Oxide Signaling Pathways Do Not Modulate *Egr2* mRNA Expression—We and others have previously shown that NO signaling is involved in the osteogenic responses of bones to mechanical loading (2–5). To determine whether *Egr2* expression is downstream of NO signaling, we treated UMR106 cells with an NO donor (SNAP2, 100 μM) for 1 h. SNAP2 treatment had no effect on *Egr2* mRNA expression levels (Fig. 8A) but increased heme oxygenase (*Ho-1*) mRNA expression after 2 h (Fig. 8B) in line with previous reports (33).

Estrogen Signaling Pathways Do Not Modulate *Egr2* mRNA Expression—There is evidence that although estrogen cooperates with prostacyclin to induce osteogenic responses to strain in rat ulnae, this does not occur with PGE2 (34). Interaction between the estrogen and prostaglandin pathways has been shown to occur during adaptive remodeling, because strain-related increases in COX2 can be blocked by ICI 182,780 treatment (35).

Given these observations and those of ourselves and others (10, 16, 25, 35) regarding the involvement of estrogen receptor α in the adaptive response of osteoblasts to mechanical strain,

EGR2 in Loading-related Gene Regulation in Bone Cells

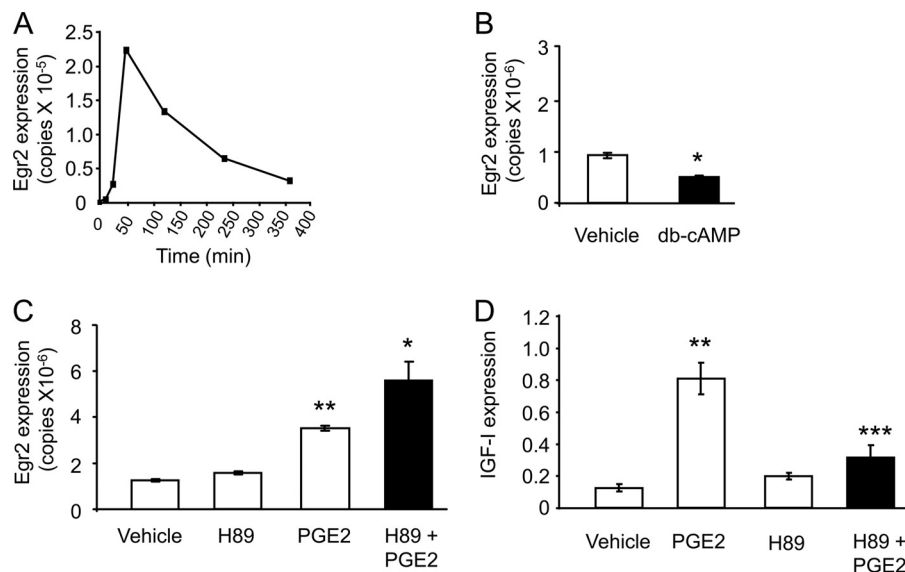


FIGURE 7. Effect of PKC and PKA signaling pathways on PGE2-induced *Egr2* mRNA expression. *A*, UMR106 cells were seeded on 66-mm dishes and treated with 500 nM PMA (PKC agonist). Total RNA was extracted 0, 10, 20, and 50 min and 2, 4, and 6 h after treatment, and RT-qPCR was used to measure normalized *Egr2* mRNA expression levels. *B*, UMR106 cells were seeded on 66-mm plastic dishes and treated with dibutyryl cyclic AMP (*db-cAMP*) (stable analog of cAMP). Total RNA was extracted 1 h after treatment, and RT-qPCR was used to measure normalized *Egr2* mRNA expression levels. Results are expressed as mean \pm S.E. *, $p < 0.05$ versus vehicle. UMR106 cells were seeded onto plastic strips and treated with 5 μ M PGE2 in the presence or absence of 1 μ M H89 (selective PKA inhibitor). Total RNA was extracted 1 h after strain, and RT-qPCR used to measure normalized *Egr2* (*C*) and *Igf-1* mRNA (*D*) expression levels. Results are expressed as mean \pm S.E. *, $p < 0.05$ versus PGE2; **, $p < 0.01$ versus vehicle; ***, $p < 0.001$ versus PGE2.

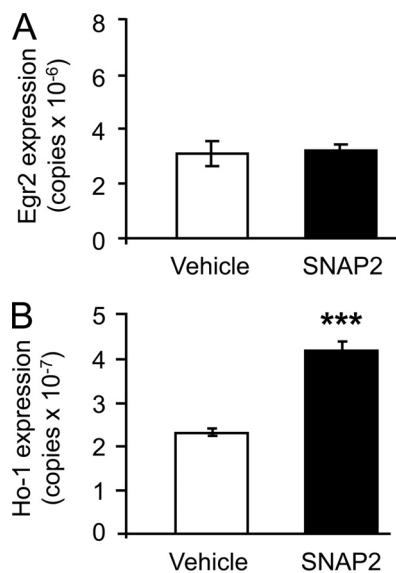


FIGURE 8. Effect of nitric oxide signaling pathways on *Egr2* mRNA expression. UMR cells were seeded onto plastic strips and treated with 100 μ M SNAP2 (NO donor). Total RNA was extracted, and RT-qPCR used to measure normalized *Egr2* (*A*) and heme oxygenase (*Ho-1*) (*B*) mRNA expression at 1 and 2 h after treatment, respectively. Results expressed as mean \pm S.E. ***, $p < 0.001$.

we sought to determine whether this pathway was involved in the regulation of *Egr2* expression. To this end, UMR106 osteoblast-like cells were treated with estrogen (10^{-8} M) and ICI 182,780 (10^{-7} M) separately, together, and in the presence or absence of PGE2 (5 μ M). Neither estrogen nor ICI 182,780, separately or together, had any effect on *Egr2* mRNA expression levels (Fig. 9A).

To determine whether regulation of the basal level of EGR2 is also dependent on ER *in vivo*, 17-week-old female C57BL/6 mice were injected daily with a subcutaneous dose of ICI 182,780 (4 mg/kg/day) for 21 days. Consistent with the

in vitro findings, *in vivo* ICI 182,780 treatment had no effect on *Egr2* mRNA expression levels (Fig. 9B). However, this is not surprising due to the observation that there are no differences in basal *Egr2* expression between nonloaded WT mice and ER $\alpha^{-/-}$ mice. To validate that the dose of ICI 182,780 used in this study was effective, we measured the uterine weights of the mice. There was a significant reduction (2.8-fold, $p < 0.001$) in the uterine weights at an ICI 182,780 dosage of 4 mg/kg/day (36).

Wnt-3a Stimulates *Egr2* mRNA Expression—Wnt/ β -catenin signaling plays an essential role in bone formation and remodeling and has been shown *in vitro* to be involved in early responses of bone cells to strain (16–18). To investigate if *Egr2* expression levels are affected by the Wnt signaling pathways, we treated UMR106 cells with recombinant Wnt-3a. Exposure of UMR106 cells to 100 ng/ml Wnt-3a resulted in significant up-regulation of *Egr2* mRNA levels (2.7-fold, $p < 0.001$) at 1 h after treatment (Fig. 10A). This behavior was replicated in primary cultures of osteoblast-like cells derived from mouse long bones. Interestingly, osteoblast-like cells similarly derived from female mice heterozygous for the G171V human high bone mass mutation maintained their strain-induced increase in *Egr2* expression for a longer period (Fig. 10B) than the osteoblast-like cells derived from their wild-type littermates (Fig. 1B). Strain-induced *Egr2* expression was not only higher in bone cells derived from these mice at 1 h after strain (3.0-fold, $p < 0.05$) but these higher levels were maintained at 3 h after strain (1.7-fold, $p < 0.05$), returning to basal levels at 6 h after treatment.

Canonical Wnt signaling is contingent on the activation of β -catenin, and we have shown previously that this can be mimicked in primary osteoblasts *in vitro* by LiCl. Interestingly, LiCl (10 mM) treatment did not affect *Egr2* mRNA expression levels in UMR106 cells (Fig. 10C), which suggests that *Egr2* transcrip-

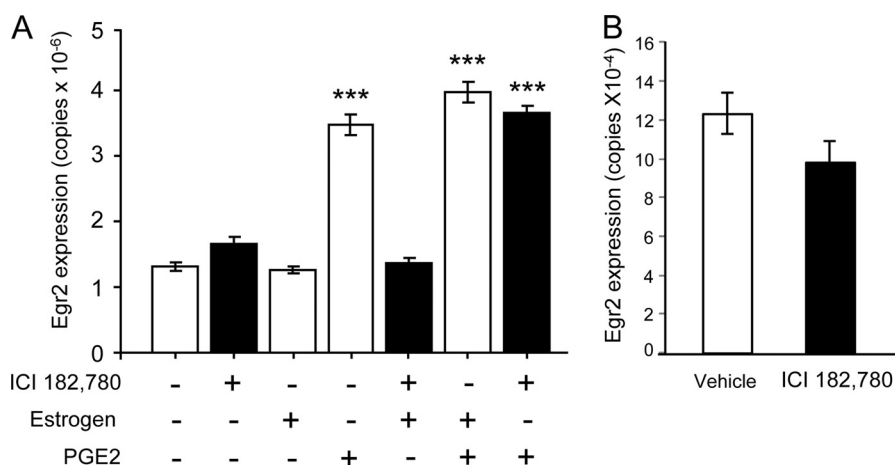


FIGURE 9. **Effect of estrogen signaling pathways on *Egr2* mRNA expression.** A, UMR106 cells were seeded on 66-mm plastic dishes and treated with 10^{-8} M estrogen, 10^{-7} M ICI 182,780 (separately and together), and $5 \mu\text{M}$ PGE2 as well as PGE2 in the presence or absence of estrogen and ICI 182,780. Total RNA was extracted 1 h after treatment, and RT-qPCR was used to measure normalized *Egr2* mRNA expression levels. Results are expressed as mean \pm S.E. ***, $p < 0.001$ versus vehicle. B, total RNA was extracted from vehicle and ICI 182,780-treated C57BL/6 mouse (subcutaneous, 4 mg/kg/day for 21 days) long bones, and RT-qPCR was used to measure *Egr2* mRNA expression levels. Results are expressed as mean \pm S.E.

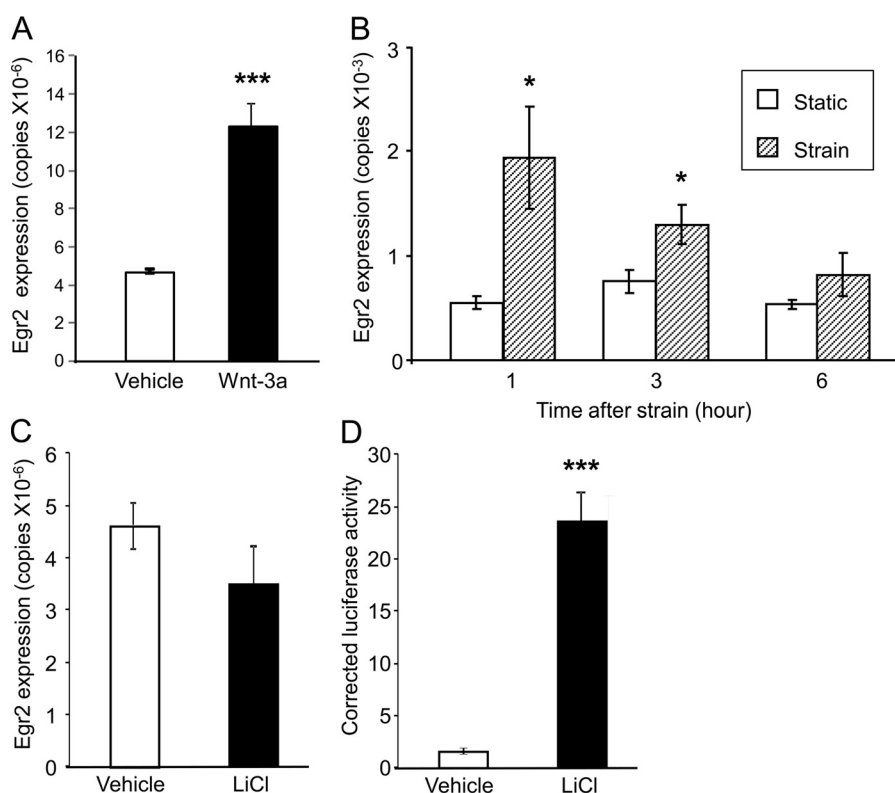


FIGURE 10. **Effect of Wnt signaling pathways on *Egr2* mRNA expression.** A, UMR106 cells were seeded on 66-mm dishes and treated with Wnt-3a (100 ng/ml). Total RNA was extracted 1 h after treatment, and RT-qPCR was used to measure normalized *Egr2* mRNA expression levels. Results are expressed as mean \pm S.E. ***, $p < 0.001$. B, LRP5^{G171V} mouse long bone-derived primary osteoblast-like cells were seeded onto plastic strips and subjected to strain. Total RNA was extracted 1, 3, and 6 h after strain, and RT-qPCR was used to measure normalized *Egr2* mRNA expression levels. Results are expressed as mean \pm S.E. *, $p < 0.05$ versus static. C, UMR106 cells were seeded on 66-mm dishes and treated with LiCl (10 mM). Total RNA was extracted 1 h after treatment, and RT-qPCR was used to measure normalized *Egr2* mRNA expression levels. Results are expressed as mean \pm S.E. D, UMR106 cells were transiently transfected with TopFlash plasmid containing six TCF/LEF-binding sites driving the expression of luciferase. A control plasmid containing *Renilla* luciferase gene under the control of a cytomegalovirus (CMV) promoter was transfected at the same time to control the transfection efficiency. Cells were treated with 10 mM LiCl and harvested 24 h later. Firefly luciferase activity was determined and normalized to *Renilla*. Data are compiled from three experiments and shown as mean \pm S.E. ***, $p < 0.005$ versus vehicle.

tion in bone cells may not be regulated by the canonical Wnt/ β -catenin signaling pathway, but possibly via alternative mechanisms, involving ERK (8, 9). To test the efficacy of the added LiCl, UMR106 cells transiently transfected with a plasmid containing six TCF/LEF-binding sites driving the expression of luciferase and a control plasmid containing *Renilla* luciferase

gene under the control of a CMV promoter to control the transfection efficiency were treated with 10 mM LiCl and harvested 24 h later. Firefly luciferase activity was determined and normalized to *Renilla*. As expected, LiCl treatment resulted in a large significant increase in corrected TopFlash reporter gene activity (23-fold, $p < 0.001$) (Fig. 10D).

EGR2 in Loading-related Gene Regulation in Bone Cells

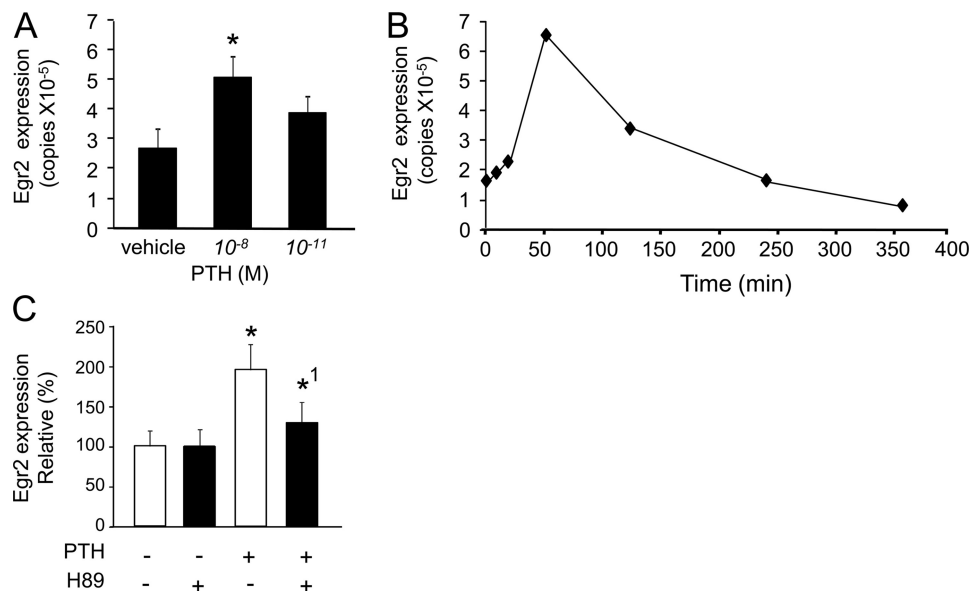


FIGURE 11. Effect of PTH on *Egr2* mRNA expression. A, UMR106 cells were seeded on 66-mm dishes and treated with PTH (10^{-8} and 10^{-10} M). Total RNA was extracted 1 h after treatment and RT-qPCR used to measure normalized *Egr2* mRNA expression levels. Results are expressed as mean \pm S.E. *, $p < 0.05$. B, UMR106 cells were seeded in tissue culture-coated dishes and treated with 10^{-8} M PTH. Total RNA was extracted 0, 10, 20, and 50 min and 2, 4, and 6 h after treatment, and RT-qPCR was used to measure normalized *Egr2* mRNA expression levels. C, UMR106 cells were treated with 10^{-8} M PTH in the presence or absence of 1 μ M H89. Total RNA was extracted 1 h after PTH treatment, and RT-qPCR was used to measure normalized *Egr2* mRNA expression levels. Results are expressed as mean \pm S.E. *, $p < 0.05$ versus vehicle; *¹, $p < 0.05$ versus PTH.

PTH-induced *Egr2* mRNA Expression—Intermittent treatment with PTH is currently the only approved anabolic treatment for osteoporosis (37). However, continuous PTH exposure associated with hyperparathyroidism results in excessive bone resorption. Models based on the UMR106 cell line by Swarthout *et al.* (38) demonstrate that low dose, but not high dose, PTH mimics these physiological phenomena *in vitro*. To establish the effect of PTH on the regulation of *Egr2* expression, we treated UMR106 cells with exogenous PTH at various concentrations. Although both the high and low concentrations of PTH (10^{-11} and 10^{-8} M, respectively) resulted in an increase in *Egr2* mRNA expression levels, only the change induced by the high concentration dose was statistically significant (1.9-fold, $p < 0.05$) (Fig. 11A). However, 10^{-8} M PTH is of the same order of magnitude as the doses we have previously used *in vivo* ($2-8 \times 10^{-8}$ M), which demonstrated an osteogenic response and, more importantly, synergized with mechanical loading to increase bone mass still further (22). The time course expression profile of *Egr2* in response to PTH (10^{-8} M) was similar to that observed with PGE2 and PMA (Fig. 11B). In contrast to enhancing PGE2-induced *Egr2* expression, H89 inhibited PTH-induced *Egr2* mRNA expression levels (Fig. 11C).

IGF-1 Induced *Egr2* mRNA Expression—A number of *in vivo* and *in vitro* studies have shown that signaling cascades induced by mechanical loading, prostaglandins, PTH, and Wnts result in expression of IGFs (15, 39–44). Because all these treatments also induce *Egr2* mRNA expression, we wanted to determine whether IGF-1 is involved in modulation of *Egr2* mRNA expression levels. Interestingly, not only did UMR106 cells exposed to IGF-1 analog (des-(1–3)-IGF-1, 50 mg/ml) show an increase in *Egr2* mRNA expression, the time course of this expression was very similar to that observed with PGE2 treatment (Fig. 12).

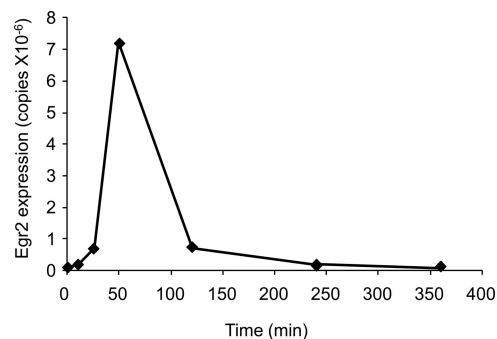


FIGURE 12. Effect of IGF-1 on *Egr2* mRNA expression. UMR106 cells were seeded on 66-mm dishes and treated with IGF-1 analog (des-(1–3)-IGF-1, 50 ng/ml). Total RNA was extracted at 0, 10, 20, and 50 min and 2, 4, and 6 h after treatment, and RT-qPCR used to measure normalized *Egr2* mRNA expression levels. Results are expressed as mean \pm S.E.

***Egr2* mRNA Expression Is Significantly Inhibited by Selective Inhibitor of MEK**—Strain, PGE2, IGF-1, Wnt-3a, and PMA not only stimulated *Egr2* mRNA expression levels but they are also known to induce ERK1/2 activation by MEK. We examined the effect of a selective MEK inhibitor (PD98059) on the regulation of *Egr2* mRNA expression levels by these agents. Pretreatment with PD98059 (30 μ M, 30 min) significantly inhibited strain (2.9-fold, $p < 0.001$), PGE2 (3.1-fold $p < 0.001$), IGF-1 (17.8-fold, $p < 0.001$), Wnt-3a (2.62-fold, $p < 0.001$), and PMA (7.2-fold, $p < 0.001$)-induced *Egr2* mRNA expression levels (Fig. 13, A–E). This suggests that strain-related regulation of *Egr2* mediated by PGs also requires activation of ERK.

***EGR2* Appears Not to Be Involved in PGE2/*Sost* Down-regulation**—Another promising anabolic treatment for osteoporosis is a sclerostin-neutralizing antibody. Sclerostin is the product of the *Sost* gene, which is a ligand for the Frizzled/LRP5 receptor and thus a regulator of the Wnt pathway (45, 46). Strain and PTH down-regulate sclerostin expression (18, 47)

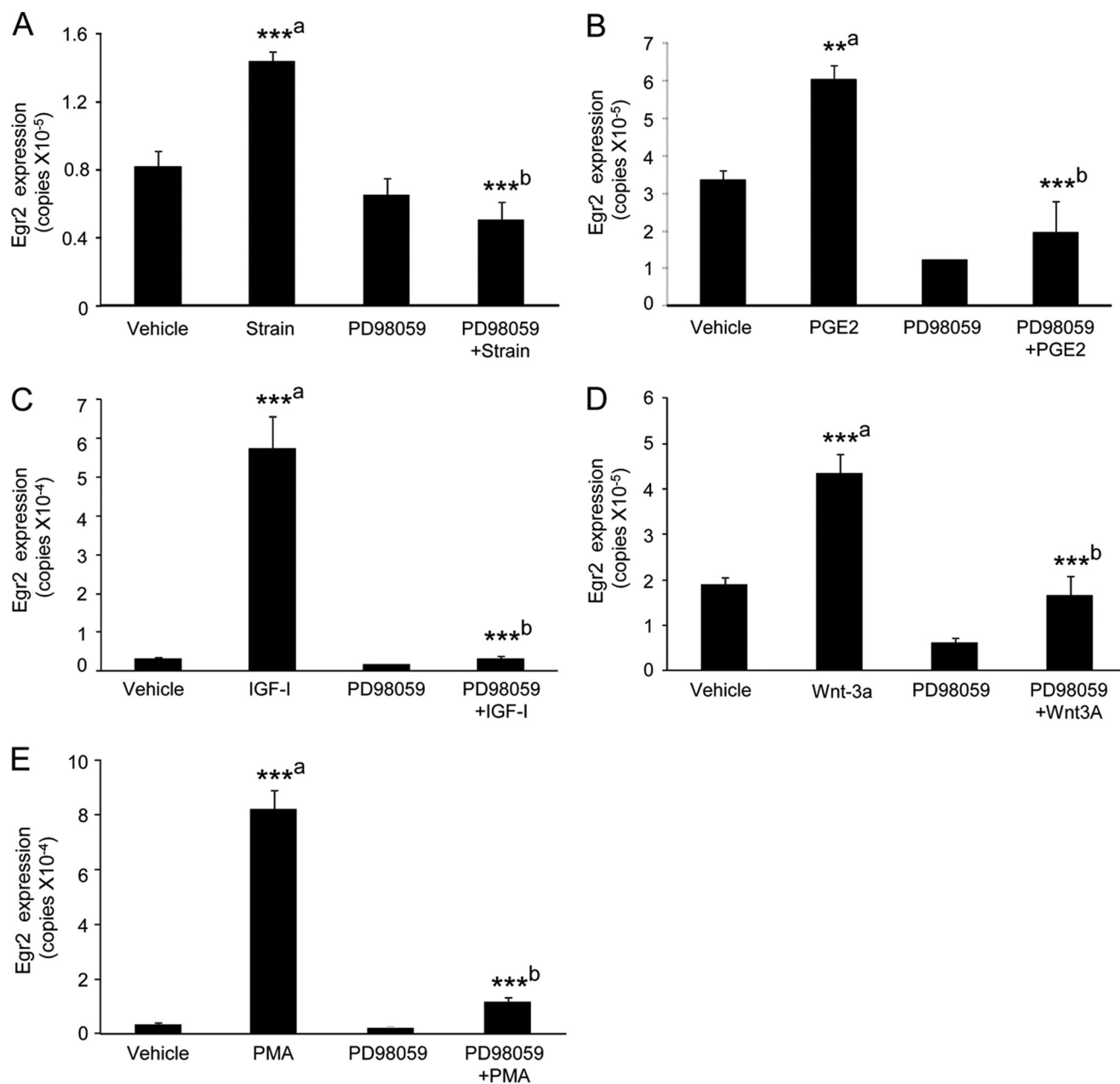


FIGURE 13. **Effect of PD98059 on strain-, PGE2-, IGF-1-, Wnt-3a-, and PMA-induced *Egr2* mRNA expression.** UMR106 cells were seeded on 66-mm dishes and treated with the following: strain (A); PGE2 (5 μ M) (B); IGF-1 (50 ng/ml) (C); Wnt-3a (100 ng/ml) (D), and PMA (500 nM) (E) in the presence and absence of PD98059 (30 μ M) pretreatment (30 min). Total RNA was extracted at 1 h after treatment, and RT-qPCR was used to measure normalized *Egr2* mRNA expression levels. Results are expressed as mean \pm S.E. **, $p < 0.01$; ***, $p < 0.001$, a = versus vehicle and b = versus treatment (strain, PGE2, IGF-1, Wnt-3a, and PMA).

through a mechanism involving COX2/PGE2 signaling (48), thus reducing competition with Wnt at the Frizzled/LRP5 receptor and so up-regulating the Wnt pathway. To establish the relationship between strain-related regulation of *Sost* and *Egr2*, we examined the effects on *Sost* mRNA expression levels of strain, PGE2, PMA, and IGF1, all of which up-regulate *Egr2*.

Of these four treatments, three resulted in down-regulation of *Sost* mRNA expression levels. Strain down-regulated *Sost* mRNA expression by 3.7-fold for 6 h ($p < 0.001$) (Fig. 14A), and exogenous treatment of both PGE2 and PMA resulted in a 49% decrease in *Sost* mRNA levels by 2 h, which was maintained at 6 h after treatment (Fig. 14B). In contrast, IGF-1 had no effect on levels of *Sost* mRNA. This discontinuity between *Egr2* and *Sost* expression lev-

els was further highlighted when the introduction of *EGR2* siRNA significantly reduced PGE2-mediated *Egr2* mRNA expression levels, but it had no effect on PGE2-mediated changes in *Sost* mRNA expression levels (Fig. 15A). The effectiveness of *EGR2* siRNA was shown by its inhibition of PGE2-mediated changes in *Oc* mRNA expression levels (Fig. 15B).

This suggests branching of the downstream pathways following PG receptor activation such that some branches stimulate *Egr2* (and *Oc*) production, whereas an *Egr2*-independent branch is involved with the down-regulation of *Sost* mRNA expression. This is consistent with our previous report that strain and PGE2 regulate *Sost* expression through an EP4-dependent pathway but regulate osteocalcin expression through EP2 (48).

EGR2 in Loading-related Gene Regulation in Bone Cells

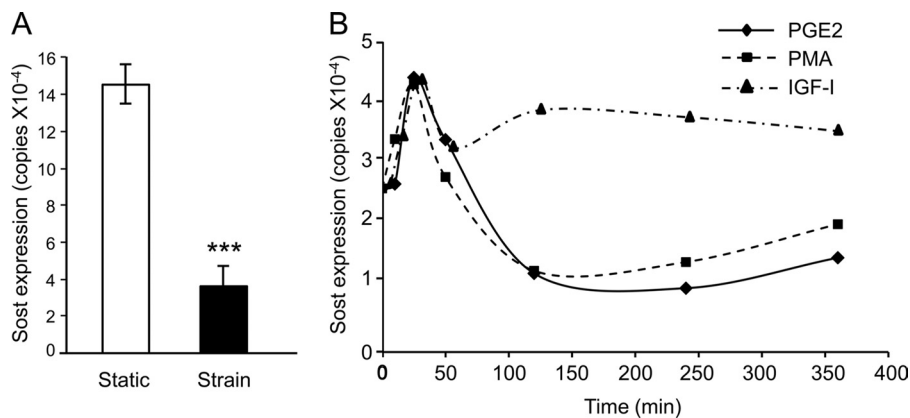


FIGURE 14. **Effect of strain, PGE2, PMA, and IGF-1 on *Sost* mRNA expression.** *A*, UMR106 cells were seeded onto plastic strips and subjected to strain. Total RNA was extracted at 15 h after strain, and normalized *Sost* mRNA expression levels were measured by RT-qPCR. Normalized *Sost* mRNA expression levels are shown compared with the static controls. Results are expressed as mean \pm S.E. ***, $p < 0.001$. *B*, UMR106 cells were seeded on 66-mm plastic dishes and treated with PGE2 (5 μ M), PMA (500 nM), and IGF-1 (50 ng/ml). Total RNA was extracted at 0, 10, 20, and 50 min and 2, 4, and 6 h after treatment, and RT-qPCR was used to measure normalized *Sost* mRNA expression levels. Results are expressed as mean \pm S.E.

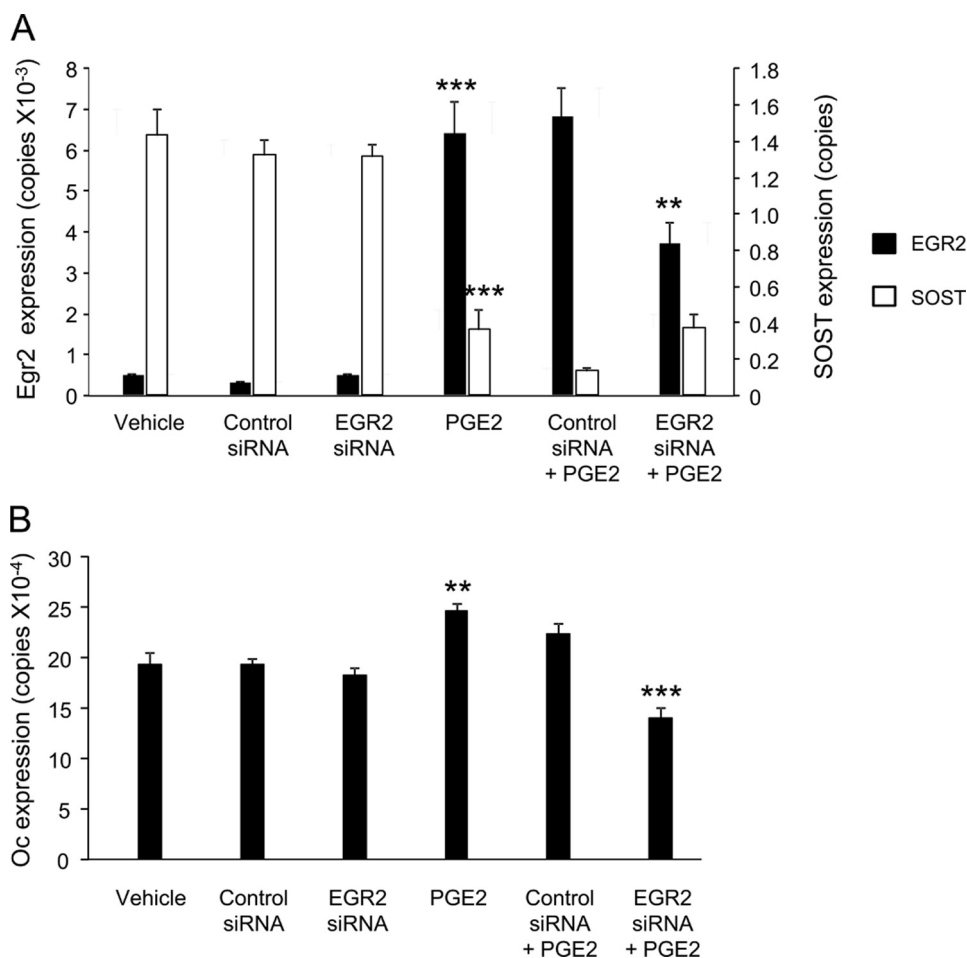


FIGURE 15. **Effect of EGR2 siRNA on PGE2-induced *Egr2*, *Sost*, and *Oc* mRNA expression.** UMR106 cells were transfected with EGR2 siRNA (100 nM), and 24 h later were treated with PGE2 (5 μ M). *A*, total RNA was extracted at 1 and 6 h after PGE2 treatment and analyzed for normalized *Egr2* and *Sost* mRNA expression levels using RT-qPCR. Results are expressed as mean \pm S.E. **, $p < 0.001$ versus vehicle. ***, $p < 0.001$ versus control siRNA and PGE2 treatment. *B*, total RNA was extracted at 4 h after PGE2 treatment and analyzed for normalized osteocalcin mRNA expression levels using RT-qPCR. Results are expressed as mean \pm S.E. **, $p < 0.001$ versus vehicle. ***, $p < 0.001$ versus control siRNA and PGE2 treatment.

DISCUSSION

In this study, we present evidence from total RNA extracted from *in vivo* loaded mouse tibiae available from our previous microarray study (19) that expression of the transcription fac-

tor EGR2 is transiently increased by loading. PASTAA analysis of data available from that study revealed that EGR2 had the highest association of any transcription factor with the genes differentially regulated by loading/unloading. The genes con-

tributing the most to the significance of EGR2's contribution were those associated with the functions of growth, proliferation, and skeletal function. Here, we also show that the *in vivo* loading-related response is replicated in strained primary cultures of osteoblast-like cells derived from murine long bones and in the UMR106 osteoblast-like cell line. Increased expression of *Egr2* by strain *in vitro* was imitated by addition of exogenous PGE2, acting primarily through the prostaglandin receptor EP1, and was attenuated by inhibitors of COX2 and prostaglandins. PGE2-induced *Egr2* mRNA expression did not require *de novo* protein synthesis. The addition of a number of ligands, previously demonstrated to play a role in the adaptive response of bone cells to strain (PGE, Wnt-3a, des-(1–3)-IGF-1, and PTH), all mimicked the strain-related increase in *Egr2* expression. In contrast, the addition of the NO donor, while stimulating *Ho-1* expression, had no effect on *Egr2*. The disintegrin echistatin had no effect on basal or strain-related levels of *Egr2*, and neither attenuation of estrogen receptor activity by ICI 182,780 nor the addition of estrogen had a significant effect on basal *Egr2* levels. *Egr2* activation by strain or ectopic ligands was dependent on ERK1/2 activation and attenuated by activation of PKA. Although both strain and PGE2 up-regulated the expression of *Egr2*, and down-regulated that of *Sost*, silencing of *Egr2* expression with siRNA while attenuating PGE-mediated changes in osteocalcin expression had no effect on that of *Sost*.

EGR2 is a transcription factor previously shown to be involved in a number of processes in a number of cell types. It plays a role in neuronal myelination (49) (it is often mutated in Charcot Marie-Tooth syndrome (50), hindbrain patterning (51–53), and macrophage function (54)) and is activated in wound healing (55), excitotoxic shock in neuronal tissue (56), and alveolar macrophage challenge by small particles (57). Mice lacking both *Egr2* alleles display low bone mass, suggesting a significant role in skeletal homeostasis (20, 58).

That EGR2 is a component of bone cell's response to mechanical strain in bone has been shown previously in a microarray study by Ott *et al.* (21) and is supported by observations that its expression is attenuated by glucocorticoids that are potent inhibitors of adaptive remodeling (59–61). With regard to the adaptive response of bone to mechanical loading, the key question that we wished to address is its role in the pathways known to function in cells of the osteoblast/osteocyte lineage within the first few minutes after exposure to mechanical stimulation. In this regard, it was fortunate that cells of the UMR106 osteoblastic cell line appear to exhibit *in vitro* similar strain-related responses in *Egr2* expression to primary cultures of osteoblast-like cells extracted from mouse long bones. These cells in turn appear to replicate loading-related changes in *Egr2* expression in whole bones loaded *in vivo*. Recently, Mantila Roosa *et al.* (62) in another microarray study have also reported modulation of the mRNA expression in early growth response genes (*Egr-1* and *Egr-3*) in response to mechanical loading *in vivo*.

Ligands Capable of Activating *Egr2* Expression—The ability of mechanical strain in UMR106 cells to activate *Egr2* mRNA expression in the presence of the disintegrin echistatin was unaltered suggesting that the initiating event in the pathways of mechanical responsiveness of the cells involving EGR2 is only

partly mediated by the $\beta 1$ and $\beta 3$ integrin attachments of the cells.

The capacity of the COX2-selective inhibitor NS398 to block strain-induced activation of *Egr2* expression, combined with the ability of PGE2 to mimic increased *Egr2* expression, supports the involvement of prostaglandins that appear to act through the EP1 receptor. Bone cells are known to express a number of prostaglandins. Although in this study PGE2 significantly stimulated *Egr2* mRNA expression levels, other prostaglandins might have different effects from that of PGE2.

Signaling by nitric oxide is intimately connected to that of prostaglandins (4) and lies within the same early time frame, but it seems not to be involved in this response because the NO donor SNAP2, while stimulating the expression of *Ho-1*, has no effect on that of *Egr2*. Similarly, neither the inhibition of ER α with ICI 182,780 nor the addition of E2 had any effect on the basal levels of *Egr2* or the ability of PG to up-regulate it. This result is in contrast to the data from the previous microarray study that suggested that absence of ER was associated with lack of up-regulation of *Egr2 in vivo* (19). In contrast, both the ligands des-(1–3)-IGF-1 and Wnt-3a, but not LiCl *in vitro*, stimulated *Egr2* expression. Both of these have been shown to act in the early stages of the osteogenic response to strain. Taken together, these data suggest that strain-related regulation of *Egr2* expression involves prostaglandins, the IGF-1 axis, and elements of the Wnt pathway, but, in these cells at least, does not involve NO or estrogen receptor signaling. Like strain and prostaglandins, PTH stimulates *Egr2* up-regulation and down-regulates that of sclerostin. However, interference with *Egr2* regulation with siRNA has no effect on PG-mediated regulation of *Sost*, although it inhibits PG-mediated increase in osteocalcin production. The picture presented by these data is of a complex set of inter-related strain-responsive pathways, and in some *Egr2* is a key component and in others it is a nonparticipant.

Intracellular Signaling Pathways That Activate *Egr2* mRNA Expression—The extracellular ligands PGE2, des-(1–3)-IGF-1 and Wnt-3a were all able to mimic the increased expression of *Egr2* mRNA following strain. However, it remains unclear by what signal transduction pathway these ligands function to regulate *Egr2* expression. The PG receptors are G-protein-coupled receptors, which gives them the ability to activate both the protein kinase C and A pathways. The PTH receptor is similar to the prostaglandin receptors in that they are G-protein-coupled receptors capable of activating both PKA and PKC, but the mechanisms underlying the osteogenic effect of PTH are complex. Experiments *in vivo* suggest that some anabolic effects of PTH in osteoblasts are mediated via PKA-dependent pathways which, while causing osteoblasts to withdraw from the cell cycle, promotes both osteoblast survival and differentiation. By this means, they serve to increase the number of osteoblasts capable of depositing the mineralized matrix necessary to increase bone mass in the whole animal (63). However, PTH also stimulates the activation of the PKC pathway (38). By using PMA to transiently stimulate PKC, we found that this mimicked strain and PGE2-mediated activation of *Egr2*. However, when we used the PKA activator dibutyryl cyclic AMP, we found that this blocked the activation of *Egr2* expression by

PGE2. This suggests that *Egr2* transcription is activated by PKC and repressed by PKA. This inference is supported by the PGE2-mediated increase in stimulation of *Egr2* expression that we observed when cells were treated with the PKA inhibitor H89. This is consistent with the findings of Ott *et al.* (21) that H89 stimulates strain-mediated activation of *Egr2* and other immediate early genes. In contrast to the enhancing effect of H89 on PGE2-mediated *Egr2* expression, the PKA signaling inhibitor inhibited PTH-induced *Egr2* expression levels. These data suggest that although the PGE2 effects on *Egr2* expression may be channeled through PKC signaling, the effects of PTH on *Egr2* expression may be mediated more through PKA signaling.

Egr-2 Transcription Requires the MEK-1/ERK Pathway—In addition to strain, all the ligands we have demonstrated to activate *Egr2* expression, as well as activation of the PKC pathway, stimulate the ERK1/2 MAPK pathways. Our demonstration that inhibition of ERK1/2 by the MEK-1-selective antagonist PD98059 blocks the induction of *Egr2* by mechanical strain, PGE2, des-(1–3)-IGF-1, and Wnt-3a suggests that ERK1/2 signaling is a prerequisite for *Egr2* transcription.

Mechanism of Wnt Signaling in Early Stages of the Mechanical Strain Response—We have previously reported that the activation of β -catenin by mechanical strain in bone cells is contingent on the presence of ER α and signaling by both NO and IGF-1R (16, 42). Furthermore, we have presented evidence that the repression of GSK3 β , which triggers β -catenin activation during the early stages of the adaptive response, is dependent on AKT and not Wnt. Our observation shown here that treatment with Wnt-3a, but not the potent GSK-3 β inhibitor LiCl, elevates basal *Egr2* levels suggests that Frizzled/LRP5 receptor/Wnt-mediated control of *Egr2* expression is independent of canonical signaling via β -catenin. This hypothesis is supported by our observations that inhibition of ER α and NO signaling, although essential for strain-mediated β -catenin activation, has no effect on *Egr2* expression. Our data demonstrating that inhibition of MEK-1/ERK1/2 blocks Wnt-3a stimulation of *Egr2* expression support this inference and suggest that the roles for Wnts and β -catenin signaling in the adaptive response of osteoblasts to mechanical strain are even more complicated than previously thought. This also agrees with our observation that the *Egr2* response to mechanical strain was exaggerated in osteoblasts isolated from high bone mass mice expressing the G171V activating mutation in LRP5 suggesting that enhanced/prolonged Wnt signaling involving *Egr2* may be acting via ERK rather than β -catenin.

Role of ERK in Egr2 Regulation—We and others (8, 64) have demonstrated the importance of ERK1/2 in bone cell response to mechanical strain and especially its role in association with ER α signaling that is critical to the adaptive response. Plotkin *et al.* (64) have proposed a model in which the assembly of a multiprotein complex on the cell surface called the signalosome is necessary for ERK1/2 activation and subsequent propagation of adaptive remodeling. Although we have not demonstrated the presence of the signalosome, we have shown that activation of *Egr2* expression by strain, PGE2, Wnt, and des-(1–3)-IGF-1 are all dependent on ERK1/2 signaling.

Role of Signal Transduction Pathway Cross-talk in Response of Osteoblasts to Mechanical Strain—The data presented here suggest that the immediate early gene *Egr2* is a nexus for ERK1/2 signaling mediated by mechanical strain, PG, IGF, and Wnt signaling. However, the role of *Egr2* in the strain response is unclear. Silencing of EGR2 has no apparent effect on the expression of *Sost*, a repressor of Wnt signaling that is thought to be a key constituent of the osteogenic response to strain, suggesting that the various combinations of inputs into the cell that compose mechanical strain signaling (PG, IGF-1, etc.) result in activation of a number of pathways in some of which *Egr2* is up-regulated but in others it is not. This reinforces our previous assertion regarding the nature of the signaling involved in the adaptive osteogenic response to strain, namely that there is no unique receptor or pathway by which bone cells process strain-related information to control bone (re)modeling. Instead, it seems that the cells immediately exposed to strain and its immediate consequences (the osteocytes and osteoblasts) assemble their strain-related stimulus for adaptive (re)modeling through the interplay of a number of ubiquitous pathways, none of which are unique to either bone or to strain. The outcome, in terms of command stimuli for bone formation, resorption, or maintenance of the architectural status quo, will be the result of the interaction of these pathways. The activity of these pathways will also be influenced by numerous other factors derived from other features of their context. In such a model, isolated regulation of some of the many inputs (e.g. PG but not canonical β -catenin signaling) will affect some but not all of the outputs (*Egr2* but not *Sost*).

It is clear from the data presented here that EGR2 is a component of strain-sensitive pathways that also involve ERK1/2, PG, IGF-1, Wnt, and PTH. The particular role of EGR2 and the identity of the EGR2 targets that act as effectors for the control of adaptive bone (re)modeling remain to be determined.

REFERENCES

1. Frost, H. M. (1987) The mechanostat: a proposed pathogenic mechanism of osteoporosis and the bone mass effects of mechanical and nonmechanical agents. *Bone Miner.* **2**, 73–85
2. Bakker, A. D., Klein-Nulend, J., Tanck, E., Albers, G. H., Lips, P., and Burger, E. H. (2005) Additive effects of estrogen and mechanical stress on nitric oxide and prostaglandin E2 production by bone cells from osteoporotic donors. *Osteoporos Int.* **16**, 983–989
3. Chow, J. W., Fox, S. W., Lean, J. M., and Chambers, T. J. (1998) Role of nitric oxide and prostaglandins in mechanically induced bone formation. *J. Bone Miner. Res.* **13**, 1039–1044
4. Pitsillides, A. A., Rawlinson, S. C., Suswillo, R. F., Bourrin, S., Zaman, G., and Lanyon, L. E. (1995) Mechanical strain-induced NO production by bone cells: a possible role in adaptive bone (re)modeling? *FASEB J.* **9**, 1614–1622
5. Zaman, G., Pitsillides, A. A., Rawlinson, S. C., Suswillo, R. F., Mosley, J. R., Cheng, M. Z., Platts, L. A., Hukkanen, M., Polak, J. M., and Lanyon, L. E. (1999) Mechanical strain stimulates nitric oxide production by rapid activation of endothelial nitric oxide synthase in osteocytes. *J. Bone Miner. Res.* **14**, 1123–1131
6. Forwood, M. R. (1996) Inducible cyclo-oxygenase (COX-2) mediates the induction of bone formation by mechanical loading in vivo. *J. Bone Miner. Res.* **11**, 1688–1693
7. Li, J., Burr, D. B., and Turner, C. H. (2002) Suppression of prostaglandin synthesis with NS-398 has different effects on endocortical and periosteal bone formation induced by mechanical loading. *Calcif. Tissue Int.* **70**, 320–329

8. Jessop, H. L., Rawlinson, S. C., Pitsillides, A. A., and Lanyon, L. E. (2002) Mechanical strain and fluid movement both activate extracellular regulated kinase (ERK) in osteoblast-like cells but via different signaling pathways. *Bone* **31**, 186–194
9. Aguirre, J. I., Plotkin, L. I., Gortazar, A. R., Millan, M. M., O'Brien, C. A., Manolagas, S. C., and Bellido, T. (2007) A novel ligand-independent function of the estrogen receptor is essential for osteocyte and osteoblast mechanotransduction. *J. Biol. Chem.* **282**, 25501–25508
10. Damien, E., Price, J. S., and Lanyon, L. E. (1998) The estrogen receptor's involvement in osteoblasts' adaptive response to mechanical strain. *J. Bone Miner. Res.* **13**, 1275–1282
11. Zaman, G., Cheng, M. Z., Jessop, H. L., White, R., and Lanyon, L. E. (2000) Mechanical strain activates estrogen response elements in bone cells. *Bone* **27**, 233–239
12. Cheng, M., Zaman, G., Rawlinson, S. C., Mohan, S., Baylink, D. J., and Lanyon, L. E. (1999) Mechanical strain stimulates ROS cell proliferation through IGF-II and estrogen through IGF-I. *J. Bone Miner. Res.* **14**, 1742–1750
13. Damien, E., Price, J. S., and Lanyon, L. E. (2000) Mechanical strain stimulates osteoblast proliferation through the estrogen receptor in males as well as females. *J. Bone Miner. Res.* **15**, 2169–2177
14. Visconti, L. A., Yen, E. H., and Johnson, R. B. (2004) Effect of strain on bone nodule formation by rat osteogenic cells in vitro. *Arch. Oral Biol.* **49**, 485–492
15. Zaman, G., Suswillo, R. F., Cheng, M. Z., Tavares, I. A., and Lanyon, L. E. (1997) Early responses to dynamic strain change and prostaglandins in bone-derived cells in culture. *J. Bone Miner. Res.* **12**, 769–777
16. Armstrong, V. J., Muzylak, M., Sunters, A., Zaman, G., Saxon, L. K., Price, J. S., and Lanyon, L. E. (2007) Wnt/ β -catenin signaling is a component of osteoblastic bone cell early responses to load-bearing and requires estrogen receptor α . *J. Biol. Chem.* **282**, 20715–20727
17. Lau, K. H., Kapur, S., Kesavan, C., and Baylink, D. J. (2006) Up-regulation of the Wnt, estrogen receptor, insulin-like growth factor-I, and bone morphogenetic protein pathways in C57BL/6J osteoblasts as opposed to C3H/HeJ osteoblasts in part contributes to the differential anabolic response to fluid shear. *J. Biol. Chem.* **281**, 9576–9588
18. Robling, A. G., Niziolek, P. J., Baldrige, L. A., Condon, K. W., Allen, M. R., Alam, I., Mantila, S. M., Gluhak-Heinrich, J., Bellido, T. M., Harris, S. E., and Turner, C. H. (2008) Mechanical stimulation of bone *in vivo* reduces osteocyte expression of Sost/sclerostin. *J. Biol. Chem.* **283**, 5866–5875
19. Zaman, G., Saxon, L. K., Sunters, A., Hilton, H., Underhill, P., Williams, D., Price, J. S., and Lanyon, L. E. (2010) Loading-related regulation of gene expression in bone in the contexts of estrogen deficiency, lack of estrogen receptor alpha and disuse. *Bone* **46**, 628–642
20. Levi, G., Topilko, P., Schneider-Maunoury, S., Lasagna, M., Mantero, S., Cancedda, R., and Charnay, P. (1996) Defective bone formation in Krox-20 mutant mice. *Development* **122**, 113–120
21. Ott, C. E., Bauer, S., Manke, T., Ahrens, S., Rödelsperger, C., Grünhagen, J., Kornak, U., Duda, G., Mundlos, S., and Robinson, P. N. (2009) Promiscuous and depolarization-induced immediate-early response genes are induced by mechanical strain of osteoblasts. *J. Bone Miner. Res.* **24**, 1247–1262
22. Sugiyama, T., Saxon, L. K., Zaman, G., Moustafa, A., Sunters, A., Price, J. S., and Lanyon, L. (2008) Mechanical loading enhances the anabolic effects of intermittent parathyroid hormone (1–34) on trabecular and cortical bone in mice. *Bone* **43**, 238–248
23. Sugiyama, T., Price, J. S., and Lanyon, L. E. (2010) Functional adaptation to mechanical loading in both cortical and cancellous bone is controlled locally and is confined to the loaded bones. *Bone* **46**, 314–321
24. Zheng, B., and Clemmons, D. R. (1998) Blocking ligand occupancy of the α v β 3 integrin inhibits insulin-like growth factor I signaling in vascular smooth muscle cells. *Proc. Natl. Acad. Sci. U.S.A.* **95**, 11217–11222
25. Zaman, G., Jessop, H. L., Muzylak, M., De Souza, R. L., Pitsillides, A. A., Price, J. S., and Lanyon, L. L. (2006) Osteocytes use estrogen receptor alpha to respond to strain but their ERalpha content is regulated by estrogen. *J. Bone Miner. Res.* **21**, 1297–1306
26. Roeder, H. G., Manke, T., O'Keefe, S., Vingron, M., and Haas, S. A. (2009) PASTAA: identifying transcription factors associated with sets of co-regulated genes. *Bioinformatics* **25**, 435–442
27. Roeder, H. G., Kanhere, A., Manke, T., and Vingron, M. (2007) Predicting transcription factor affinities to DNA from a biophysical model. *Bioinformatics* **23**, 134–141
28. Sakata, T., Wang, Y., Halloran, B. P., Elalieh, H. Z., Cao, J., and Bikle, D. D. (2004) Skeletal unloading induces resistance to insulin-like growth factor-I (IGF-I) by inhibiting activation of the IGF-I signaling pathways. *J. Bone Miner. Res.* **19**, 436–446
29. Kapur, S., Mohan, S., Baylink, D. J., and Lau, K. H. (2005) Fluid shear stress synergizes with insulin-like growth factor-I (IGF-I) on osteoblast proliferation through integrin-dependent activation of IGF-I mitogenic signaling pathway. *J. Biol. Chem.* **280**, 20163–20170
30. Plow, E. F., Haas, T. A., Zhang, L., Loftus, J., and Smith, J. W. (2000) Ligand binding to integrins. *J. Biol. Chem.* **275**, 21785–21788
31. Bellido, T. (2010) Antagonistic interplay between mechanical forces and glucocorticoids in bone: a tale of kinases. *J. Cell. Biochem.* **111**, 1–6
32. Hynes, R. O. (1999) Cell adhesion: old and new questions. *Trends Cell Biol.* **9**, M33–M37
33. Hara, E., Takahashi, K., Tominaga, T., Kumabe, T., Kayama, T., Suzuki, H., Fujita, H., Yoshimoto, T., Shirato, K., and Shibahara, S. (1996) Expression of heme oxygenase and inducible nitric-oxide synthase mRNA in human brain tumors. *Biochem. Biophys. Res. Commun.* **224**, 153–158
34. Cheng, M. Z., Zaman, G., and Lanyon, L. E. (1994) Estrogen enhances the stimulation of bone collagen synthesis by loading and exogenous prostacyclin, but not prostaglandin E2, in organ cultures of rat ulnae. *J. Bone Miner. Res.* **9**, 805–816
35. Liedert, A., Wagner, L., Seefried, L., Ebert, R., Jakob, F., and Ignatius, A. (2010) Estrogen receptor and Wnt signaling interact to regulate early gene expression in response to mechanical strain in osteoblastic cells. *Biochem. Biophys. Res. Commun.* **394**, 755–759
36. Sugiyama, T., Galea, G. L., Lanyon, L. E., and Price, J. S. (2010) Mechanical loading-related bone gain is enhanced by tamoxifen but unaffected by fulvestrant in female mice. *Endocrinology* **151**, 5582–5590
37. Debiais, F. (2003) Efficacy data on teriparatide (parathyroid hormone) in patients with postmenopausal osteoporosis. *Joint Bone Spine* **70**, 465–470
38. Swarthout, J. T., D'Alonzo, R. C., Selvamurugan, N., and Partridge, N. C. (2002) Parathyroid hormone-dependent signaling pathways regulating genes in bone cells. *Gene* **282**, 1–17
39. Chambers, T. J., Fox, S., Jagger, C. J., Lean, J. M., and Chow, J. W. (1999) The role of prostaglandins and nitric oxide in the response of bone to mechanical forces. *Osteoarthritis Cartilage* **7**, 422–423
40. Lean, J. M., Jagger, C. J., Chambers, T. J., and Chow, J. W. (1995) Increased insulin-like growth factor I mRNA expression in rat osteocytes in response to mechanical stimulation. *Am. J. Physiol.* **268**, E318–E327
41. Rawlinson, S. C., Mohan, S., Baylink, D. J., and Lanyon, L. E. (1993) Exogenous prostacyclin, but not prostaglandin E2, produces similar responses in both G6PD activity and RNA production as mechanical loading, and increases IGF-II release, in adult cancellous bone in culture. *Calcif. Tissue Int.* **53**, 324–329
42. Sunters, A., Armstrong, V. J., Zaman, G., Kypta, R. M., Kawano, Y., Lanyon, L. E., and Price, J. S. (2010) Mechano-transduction in osteoblastic cells involves strain-regulated estrogen receptor alpha-mediated control of insulin-like growth factor (IGF) I receptor sensitivity to ambient IGF, leading to phosphatidylinositol 3-kinase/AKT-dependent Wnt/LRP5 receptor-independent activation of beta-catenin signaling. *J. Biol. Chem.* **285**, 8743–8758
43. Watson, P., Lazowski, D., Han, V., Fraher, L., Steer, B., and Hodsmann, A. (1995) Parathyroid hormone restores bone mass and enhances osteoblast insulin-like growth factor I gene expression in ovariectomized rats. *Bone* **16**, 357–365
44. Yoon, J. C., Ng, A., Kim, B. H., Bianco, A., Xavier, R. J., and Elledge, S. J. (2010) Wnt signaling regulates mitochondrial physiology and insulin sensitivity. *Genes Dev.* **24**, 1507–1518
45. Baron, R., Rawadi, G., and Roman-Roman, S. (2006) Wnt signaling: a key regulator of bone mass. *Curr. Top. Dev. Biol.* **76**, 103–127
46. Winkler, D. G., Sutherland, M. S., Ojala, E., Turcott, E., Geoghegan, J. C., Shpektor, D., Skonier, J. E., Yu, C., and Latham, J. A. (2005) Sclerostin inhibition of Wnt-3a-induced C3H10T1/2 cell differentiation is indirect

- and mediated by bone morphogenetic proteins. *J. Biol. Chem.* **280**, 2498–2502
47. Moustafa, A., Sugiyama, T., Saxon, L. K., Zaman, G., Sunter, A., Armstrong, V. J., Javaheri, B., Lanyon, L. E., and Price, J. S. (2009) The mouse fibula as a suitable bone for the study of functional adaptation to mechanical loading. *Bone* **44**, 930–935
48. Galea, G. L., Sunter, A., Meakin, L. B., Zaman, G., Sugiyama, T., Lanyon, L. E., and Price, J. S. (2011) Sost down-regulation by mechanical strain in human osteoblastic cells involves PGE2 signaling via EP4. *FEBS Lett.* **585**, 2450–2454
49. Warner, L. E., Mancias, P., Butler, I. J., McDonald, C. M., Keppen, L., Koob, K. G., and Lupski, J. R. (1998) Mutations in the early growth response 2 (EGR2) gene are associated with hereditary myelinopathies. *Nat. Genet.* **18**, 382–384
50. Bellone, E., Di Maria, E., Soriani, S., Varese, A., Doria, L. L., Ajmar, F., and Mandich, P. (1999) A novel mutation (D305V) in the early growth response 2 gene is associated with severe Charcot–Marie–Tooth type 1 disease. *Hum. Mutat.* **14**, 353–354
51. Nonchev, S., Maconochie, M., Vesque, C., Aparicio, S., Ariza-McNaughton, L., Manzanares, M., Maruthinar, K., Kuroiwa, A., Brenner, S., Charnay, P., and Krumlauf, R. (1996) The conserved role of Krox-20 in directing Hox gene expression during vertebrate hindbrain segmentation. *Proc. Natl. Acad. Sci. U.S.A.* **93**, 9339–9345
52. Schneider-Maunoury, S., Topilko, P., Seitandou, T., Levi, G., Cohen-Tannoudji, M., Pournin, S., Babinet, C., and Charnay, P. (1993) Disruption of Krox-20 results in alteration of rhombomeres 3 and 5 in the developing hindbrain. *Cell* **75**, 1199–1214
53. Walshe, J., Maroon, H., McGonnell, I. M., Dickson, C., and Mason, I. (2002) Establishment of hindbrain segmental identity requires signaling by FGF3 and FGF8. *Curr. Biol.* **12**, 1117–1123
54. Hirano, S., Anuradha, C. D., and Kanno, S. (2002) krox-20/egr-2 is up-regulated following non-specific and homophilic adhesion in rat macrophages. *Immunology* **107**, 86–92
55. Grose, R., Harris, B. S., Cooper, L., Topilko, P., and Martin, P. (2002) Immediate early genes krox-24 and krox-20 are rapidly up-regulated after wounding in the embryonic and adult mouse. *Dev. Dyn.* **223**, 371–378
56. Gass, P., Katsura, K., Zuschratter, W., Siesjö, B., and Kiessling, M. (1995) Hypoglycemia-elicited immediate early gene expression in neurons and glia of the hippocampus: novel patterns of FOS, JUN, and KROX expression following excitotoxic injury. *J. Cereb. Blood Flow Metab.* **15**, 989–1001
57. Hirano, S., Anuradha, C. D., and Kanno, S. (2000) Transcription of krox-20/egr-2 is upregulated after exposure to fibrous particles and adhesion in rat alveolar macrophages. *Am. J. Respir. Cell Mol. Biol.* **23**, 313–319
58. Levi, G., Topilko, P., Schneider-Maunoury, S., Lasagna, M., Mantero, S., Pesce, B., Gherzi, G., Cancedda, R., and Charnay, P. (1996) Role of Krox-20 in endochondral bone formation. *Ann. N.Y. Acad. Sci.* **785**, 288–291
59. Leclerc, N., Luppen, C. A., Ho, V. V., Nagpal, S., Hacia, J. G., Smith, E., and Frenkel, B. (2004) Gene expression profiling of glucocorticoid-inhibited osteoblasts. *J. Mol. Endocrinol.* **33**, 175–193
60. Leclerc, N., Noh, T., Cogan, J., Samarawickrama, D. B., Smith, E., and Frenkel, B. (2008) Opposing effects of glucocorticoids and Wnt signaling on Krox20 and mineral deposition in osteoblast cultures. *J. Cell. Biochem.* **103**, 1938–1951
61. Leclerc, N., Noh, T., Khokhar, A., Smith, E., and Frenkel, B. (2005) Glucocorticoids inhibit osteocalcin transcription in osteoblasts by suppressing Egr2/Krox20-binding enhancer. *Arthritis Rheum.* **52**, 929–939
62. Mantila Roosa, S. M., Liu, Y., and Turner, C. H. (2011) Gene expression patterns in bone following mechanical loading. *J. Bone Miner. Res.* **26**, 100–112
63. Jilka, R. L. (2007) Molecular and cellular mechanisms of the anabolic effect of intermittent PTH. *Bone* **40**, 1434–1446
64. Plotkin, L. I., Mathov, I., Aguirre, J. I., Parfitt, A. M., Manolagas, S. C., and Bellido, T. (2005) Mechanical stimulation prevents osteocyte apoptosis: requirement of integrins, Src kinases, and ERKs. *Am. J. Physiol. Cell Physiol* **289**, C633–C643